

Parallel Approaches to Mono- and Bis-Propargylic Activation via $\text{Co}_2(\text{CO})_8$ and $[\text{Ru}_3(\mu\text{-Cl})(\text{CO})_{10}]^-$

Michèle Soleilhavoup, Catherine Saccavini, Christine Lepetit, Guy Lavigne,
Luc Maurette, Bruno Donnadieu, and Remi Chauvin*

Laboratoire de Chimie de Coordination du CNRS, 205 Route de Narbonne,
31077 Toulouse Cedex 4, France

Received June 26, 2001

Butyne derivatives $\text{CH}_3\text{C}\equiv\text{CCH}_2\text{X}$ and $\text{XCH}_2\text{C}\equiv\text{CCH}_2\text{X}$ (X = hydroxy, acetoxy, tosyloxy) were reacted with $\text{Co}_2(\text{CO})_8$ and $[\text{PPN}][\text{Ru}_3(\mu\text{-Cl})(\text{CO})_{10}]$. Whereas dissociation of hydroxy and acetoxy groups from the cluster-bound mono-oxypropargylic ligands $\text{CH}_3\text{C}\equiv\text{CCH}_2\text{X}$ requires the assistance of an acid, spontaneous dissociation occurs with a tosyloxy group. For cobalt, this produces the ether complex $\{\text{Co}_2(\text{CO})_6\}_2(\mu\text{-CH}_3\text{C}\equiv\text{CCH}_2\text{OCH}_2\text{C}\equiv\text{CCH}_3)$. For ruthenium, stepwise propargylic activation affords the allenyl complex $\text{Ru}_3(\mu\text{-Cl})(\mu\text{-}\eta^3\text{-CH}_3\text{-CCCH}_2)(\text{CO})_9$. The elusive allenylium cobalt intermediate $[\text{Co}_2(\mu\text{-}\eta^3\text{-CH}_3\text{CCCH}_2)(\text{CO})_6]^+$ was optimized at the B3PW91/6-31G* level of theory. Analyses of frontier orbitals, Mulliken charges, and Fukui indices reveal that the ruthenium complex is less electrophilic than the cobalt complex and that soft nucleophiles should react at metal centers in both complexes. This provides a rationale for the known reactivity of Nicholas' cobalt complexes. It is also consistent with the observed reactivity of a hydride with the ruthenium complex, which takes place at the metal, followed by H transfer to the propargylic carbon. With the bis-oxypropargylic ligands, the complexes $\text{Co}_2(\mu\text{-XCH}_2\text{C}\equiv\text{CCH}_2\text{X})(\text{CO})_6$ and $[\text{Ru}_3(\mu\text{-Cl})(\mu\text{-XCH}_2\text{-C}\equiv\text{CCH}_2\text{X})(\text{CO})_9]^-$ (X = OH, OAc) were also prepared. Protonation of the latter yields the neutral allenyl species $\text{Ru}_3(\mu\text{-Cl})(\mu\text{-}\eta^3\text{-XCH}_2\text{CCCH}_2)(\text{CO})_9$. Again, the specific behavior of the bis(tosyloxy) ligand (X = OTs) was observed. While the cobalt complex $\text{Co}_2(\mu\text{-}\eta^2\text{-TsOCH}_2\text{-CCCH}_2\text{OTs})(\text{CO})_6$ turned out to be relatively stable, a butatriene-type ruthenium complex was detected by in situ 2D ^1H – ^{13}C NMR. The target cationic butatriene complex $[\text{Ru}_3(\mu\text{-Cl})(\mu\text{-}\eta^4\text{-CH}_2\text{CCCH}_2)(\text{CO})_9][\text{BF}_4]$ was finally obtained by protonation of the hydroxyallenyl complex $\text{Ru}_3(\mu\text{-Cl})(\mu\text{-}\eta^3\text{-HOCH}_2\text{CCCH}_2)(\text{CO})_9$.

Introduction

Due to their extensive practical applications in organic synthesis, alkyne–cobalt(0) complexes have received considerable attention. Indeed, the dicobalt hexacarbonyl unit is involved as a promoter in the Pauson–Khand reaction¹ and as a versatile protecting group for triple bonds,² enabling in particular the activation of Nicholas-type propargylic pseudo- $\text{S}_{\text{N}}1$ reactions.^{3,4} Within the latter prospect, many η^2 -propargylic halide, alcohol, ether, and ester complexes $\text{Co}_2(\mu\text{-}\eta^2\text{-RCCCH}_2\text{X})(\text{CO})_6$ (**Ia**) have been described (Scheme 1).⁵ Their subsequent conversion into η^3 -propargylic carbenium complexes $[\text{Co}_2(\mu\text{-}\eta^3\text{-RCCCH}_2)(\text{CO})_6]^+$ (**Ib**) depends on the nature of the leaving group: the dissociation of acetates requires the assistance of an acid,⁶ whereas related triflate complexes exist exclusively as η^3 -propargylic

carbenium salts, due to preexisting polarization of the propargylic $\text{C}^{\delta+}\text{—O}^{\delta-}\text{Tf}$ bond. Though the tosylate group might be expected to exhibit a pivotal behavior, the corresponding Nicholas-type complexes have not been intercepted.

To date, the bimetallic units $\text{Co}_2(\text{CO})_4(\text{dppm})$, $\text{Mo}_2\text{-Cp}_2(\text{CO})_4$, and $\text{CoMoCp}(\text{CO})_5$ remain the main general alternatives to the use of the $\text{Co}_2(\text{CO})_6$ unit for propargylic activation.⁷ Keeping in mind recent observations that a growing number of cobalt-specific reactions of alkynes (i.e. the Pauson–Khand reaction) are now catalyzed by $\text{Ru}_3(\text{CO})_{12}$,⁸ we became interested in examining the ability of ruthenium complexes to activate Nicholas-type propargylic substitutions. The well-established “halide promoted”⁹ reaction of alkynes with $\text{Ru}_3(\text{CO})_{12}$ appeared as a rational synthetic route to the desired trinuclear complexes $[\text{Ru}_3(\mu\text{-Cl})\text{-}\eta^2\text{-RCCCH}_2\text{X})(\text{CO})_9]^-$ (**IIa**) and $\text{Ru}_3(\mu\text{-Cl})(\mu\text{-}\eta^3\text{-RCCCH}_2)(\text{CO})_9$ (**IIb**) (Scheme 1). The comparative study is carried out in both

* To whom correspondence should be addressed. Tel: 33 (0)5 61 33 31 13. Fax: 33 (0)5 61 55 30 03. E-mail: chauvin@lcc-toulouse.fr.

(1) Shore, N. E. *Chem. Rev.* **1988**, *88*, 1081–1119.

(2) Nicholas, K. M.; Pettit, R. *Tetrahedron Lett.* **1971**, *37*, 3475–3478.

(3) Nicholas, K. M. *Acc. Chem. Res.* **1987**, *20*, 207–214.

(4) Huhn, O.; Rau, D.; Mayr, H. *J. Am. Chem. Soc.* **1998**, *120*, 900–907.

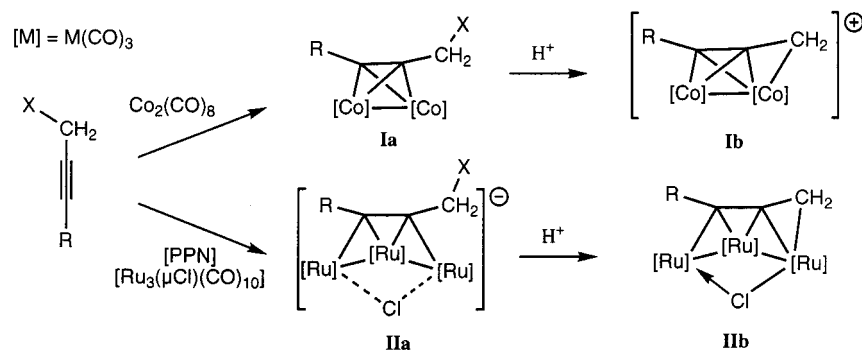
(5) Went, M. J. *Adv. Organomet. Chem.* **1997**, *41*, 69–125.

(6) When the metal counterpart of the nucleophile is sufficiently Lewis acidic (aluminum), the use of an auxiliary acid can be avoided: Padmanabhan, S.; Nicholas, K. M. *Tetrahedron Lett.* **1983**, *24*, 2239.

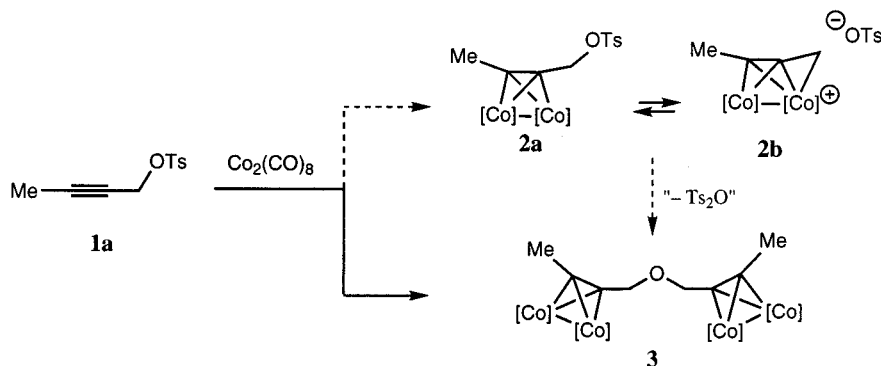
(7) (a) McGlinchey, M. J.; Girard, L.; Ruffolo, R. *Coord. Chem. Rev.* **1995**, *143*, 331–381. (b) Müller, T. J. *J. Eur. J. Inorg. Chem.* **2001**, 2021.

(8) Kondo, T.; Suzuki, N.; Okada, T.; Mitsudo, T. *J. Am. Chem. Soc.* **1997**, *119*, 6187–6188.

(9) (a) Rivomanana, S.; Lavigne, G.; Lugan, N.; Bonnet, J.-J.; Yanez, R. *J. Am. Chem. Soc.* **1989**, *111*, 8959–8960. (b) Rivomanana, S.; Lavigne, G.; Lugan, N.; Bonnet, J.-J. *J. Am. Chem. Soc.* **1990**, *112*, 8607–8609. (c) Lavigne, G. *Eur. J. Inorg. Chem.* **1999**, 917–930.

Scheme 1. Analogy between Propargyl Tricarbonylcobalt and Tricarbonylruthenium Clusters^a

^a X = oxy substituent. Note: the dotted lines represent the average of the two Lewis resonance structures with a localized minus charge and a formal 18-electron count for all the Ru atoms: $[\text{Ru}]^--\text{Cl}-[\text{Ru}] \leftrightarrow [\text{Ru}]\leftarrow\text{Cl}-[\text{Ru}]^-$.

Scheme 2. Peculiar Reactivity of 1-(Tosyloxy)but-2-yne (1a) with $\text{Co}_2(\text{CO})_8$ 

^a $[\text{Co}] = \text{Co}(\text{CO})_3$.

mono- and bis-propargylic series, using the alkyne prototypes $\text{CH}_3\text{C}\equiv\text{CCH}_2\text{X}$ and $\text{XCH}_2\text{C}\equiv\text{CCH}_2\text{X}$, respectively, with X = hydroxy, acetoxy, tosyloxy.

Results and Discussion

Monopropargylic Activation. (1) Experimental Results in the Cobalt Series. Whereas propargylic ethers, alcohols, and acetates readily react with $\text{Co}_2(\text{CO})_8$ to afford the corresponding neutral Nicholas-type complexes, the corresponding complex **2** (in either the associated form $\text{Co}_2(\mu-\eta^2\text{-CH}_3\text{CCCH}_2\text{OTs})(\text{CO})_6$ (**2a**) or dissociated form $[\text{Co}_2(\mu-\eta^3\text{-CH}_3\text{CCCH}_2)(\text{CO})_6][\text{OTs}]$ (**2b**)) could not be isolated from the reaction of 1-(tosyloxy)-but-2-yne (**1a**) with $\text{Co}_2(\text{CO})_8$. Instead, the dibutynyl ether complex **3** was isolated in 79% yield (Scheme 2).

The X-ray crystal structure of complex **3** (Figure 1 and Table 1) has to be compared with that of the isostructural alkyne complex $\{\text{Co}_2(\text{CO})_6\}_2(\mu\text{-HC}\equiv\text{CCH}_2\text{OCH}_2\text{C}\equiv\text{CH})$, previously prepared by the classical route via reaction of dipropynyl ether with $\text{Co}_2(\text{CO})_8$.¹⁰ The $\eta^2\text{-C}\equiv\text{CH}$ bonds of the latter complex were seen to be quite long. Despite the larger steric demand of the methyl substituents, the $\eta^2\text{-C}\equiv\text{CMe}$ bond lengths in **3** (1.284(13) and 1.297(13) Å) tend to be slightly shorter than the corresponding $\eta^2\text{-C}\equiv\text{CH}$ bond lengths in the homologous bis-terminal alkyne complex (1.308(6) and 1.316(6) Å) and markedly shorter than classical acetylenic $\eta^2\text{-C}\equiv\text{C}$ bonds in related cobalt complexes (in the range 1.33–1.36 Å).¹⁰ The electron-withdrawing effect

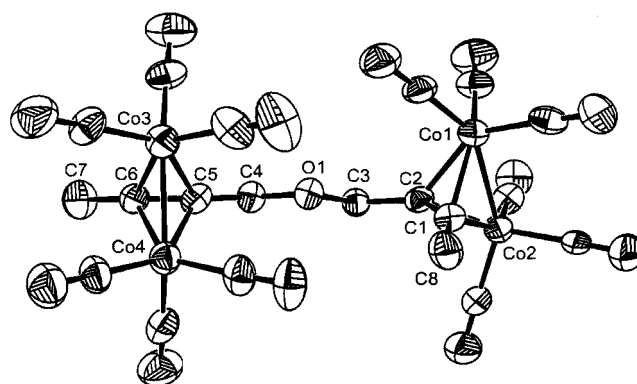


Figure 1. X-ray crystal structure of complex **3**. Selected bond distances in Å: Co(1)–Co(2) = 2.4654(18); Co(3)–Co(4) = 2.4602(19); Co(1)–C(2) = 1.934(9); Co(1)–C(1) = 1.963(9); Co(2)–C(2) = 1.924(10); Co(2)–C(1) = 1.943(9); Co(3)–C(6) = 1.927(10); Co(3)–C(5) = 1.943(9); Co(4)–C(5) = 1.931(10); Co(4)–C(6) = 1.946(10); C(1)–C(2) = 1.284(13); C(5)–C(6) = 1.297(13). Selected bond angles in deg: C(1)–C(2)–C(3) = 141.5(9); C(2)–C(1)–C(8) = 145.4(10); C(6)–C(5)–C(4) = 141.1(10); C(5)–C(6)–C(7) = 141.3(10); C(4)–O(1)–C(3) = 107.9(7).

of the $\text{Co}_2(\text{CO})_6$ units is thus lowered by a long-range inductive effect of the doubly propargylic oxygen atom.

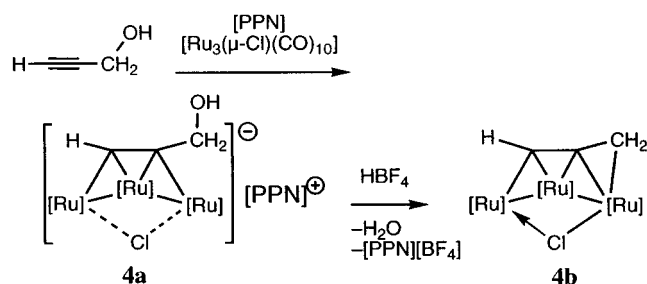
The intermediacy of a more or less dissociated form of complex **2** en route to **3** can be reasonably expected. In the absence of any detectable trace of but-2-yn-1-ol (which might result from incidental hydrolysis),¹¹ the formation of ether **3** under neutral conditions reveals a peculiar reactivity of complex **2** (Scheme 2).

(2) Experimental Results in the Ruthenium Series. It was previously noted^{9c} that the reaction of

(10) Chen, X.-N.; Zhang, J.; Wu, S.-L.; Yin, Y.-Q.; Wang, W.-L.; Sun, J. *J. Chem. Soc., Dalton Trans.* **1999**, 1987–1991.

Table 1. Crystal Data and Structure Refinement for Complexes **3**, **5b**, and **8a**^a

	3	5b	8a
formula	C ₂₁ H ₁₀ Co ₄ O ₁₃	C ₁₃ H ₅ ClO ₉ Ru ₃	C ₁₄ H ₁₀ O ₁₀ Co ₂
fw	705.74	643.83	456.08
temp (K)	180(2)	160(2)	298(2)
wavelength (Å)	0.71073	0.71073	0.71073
cryst syst	triclinic	triclinic	triclinic
space group	<i>P</i> $\bar{1}$	<i>P</i> $\bar{1}$	<i>P</i> $\bar{1}$
<i>a</i> (Å)	7.515(2)	9.443(2)	9.222(2)
<i>b</i> (Å)	10.637(2)	9.501(2)	73.30(3)
<i>c</i> (Å)	16.180(3)	10.194(2)	12.697(3)
α (deg)	94.56(3)	77.43(3)	73.30(3)
β (deg)	94.54(3)	87.03(3)	87.57(3)
γ (deg)	92.04(3)	86.13(3)	62.87(3)
<i>V</i> (Å ³)	1284.1(5)	890.0(3)	927.9(4)
<i>Z</i>	2	2	2
ρ (g cm ⁻³)	1.369	2.403	1.632
abs coeff μ (mm ⁻¹)	0.729	2.706	1.835
<i>F</i> (000)	534	608	456
θ range (deg)	1.92–23.25	2.05–25.96	2.50–25.99
index ranges	–8 ≤ <i>h</i> ≤ 8 –11 ≤ <i>k</i> ≤ 11 –17 ≤ <i>l</i> ≤ 17	–11 ≤ <i>h</i> ≤ 11 –11 ≤ <i>k</i> ≤ 11 –12 ≤ <i>l</i> ≤ 12	–11 ≤ <i>h</i> ≤ 11 –11 ≤ <i>k</i> ≤ 11 –15 ≤ <i>l</i> ≤ 15
no. of rflns			
collected	9506	8652	8486
unique	3500	3208	3373
<i>R</i> (int)	0.1061	0.0411	0.0626
completeness (%)	94.8 (to 2 θ = 23.25°)	92.2 (to 2 θ = 25.96°)	92.6 (to 2 θ = 25.99°)
no. of data	3500	3208	3373
restraints	0	0	0
params	336	236	237
<i>R</i> 1 (<i>I</i> > 2 σ (<i>I</i>))	0.0497	0.0233	0.0395
<i>wR</i> 2 (<i>I</i> > 2 σ (<i>I</i>))	0.0869	0.0582	0.0920
<i>R</i> 1 (all data)	0.1321	0.0253	0.0699
<i>wR</i> 2 (all data)	0.1103	0.0593	0.1052
$\Delta\rho_{\max}$ (e Å ⁻³)	0.462	0.626	0.319
$\Delta\rho_{\min}$ (e Å ⁻³)	–0.351	–0.678	–0.420

^a Refinement method: full-matrix least squares on *F*².**Scheme 3.** Synthesis of Propargylic Complexes **4a** and **4b**^a^a [Ru] = Ru(CO)₃.

propargyl alcohol with Ru₃(CO)₁₂ in the presence of bis-(triphenylphosphine)nitrogen(1+) chloride ([PPN][Cl]) proceeds as established earlier for terminal and internal alkynes, producing the anionic propargylic alcohol triruthenate complex **4a** (Scheme 3). As noted by Basolo,¹² the observed kinetics for complexation of alkynols are particularly fast, since the protic character of the ligand itself facilitates a transient opening of the Ru–Cl bond.

(11) Complex **3** could result from partial hydrolysis of **2** and reaction of the alcohol with another molecule of **2**. However, the absence of unreacted alcohol in the crude product (NMR) would result from an extraordinary coincidence (the amount of water would be exactly half the amount of **2**). It may also be proposed that **2** is so reactive that it even reacts with an oxygen atom of the propargyl tosyl ether **1a**, the nucleophilicity of which is generally negligible.

(12) (a) Shen, J.-K.; Basolo, F. *Gazz. Chim. Ital.* **1994**, *124*, 439. (b) Basolo, F. Private communication.

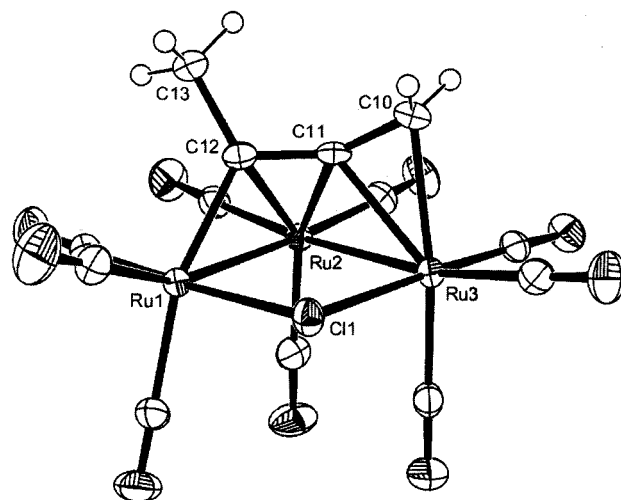


Figure 2. X-ray crystal structure of complex **5b**. Selected bond distances in Å: Ru(1)–Cl(1) = 2.4769(10); Ru(1)–Ru(2) = 2.7931(7); Ru(2)–Ru(3) = 2.8487(10); Ru(3)–Cl(1) = 2.4290(9); Ru(1)–C(12) = 2.076(3); Ru(2)–C(12) = 2.253(2); Ru(2)–C(11) = 2.095(2); Ru(3)–C(11) = 2.263(3); Ru(3)–C(10) = 2.277(3); C(12)–C(11) = 1.383(4); C(11)–C(10) = 1.380(4). Selected bond angles in deg: C(11)–C(10)–Ru(3) = 71.77(15); C(10)–C(11)–C(12) = 142.8(2); C(11)–C(12)–C(13) = 116.8(2); C(11)–C(12)–Ru(1) = 117.70(18).

Upon protonation of **4a** by HBF₄ in THF, the neutral allenyl complex **4b** was produced.^{9c,13}

When the analogous reaction was performed with 1-(tosyloxy)but-2-yne (**1a**), the expected intermediate [Ru₃(μ-Cl)(μ-η²-CH₃CCCH₂OTs)(CO)₉][–] (**5a**) (corresponding to **2a** in the cobalt series) was not detected by IR, whereas the reaction readily proceeded toward the formation of the neutral allenyl complex Ru₃(μ-Cl)(μ-η³-CH₃CCCH₂)(CO)₉ (**5b**), isolated in 68% yield (Scheme 4). This provided a hint that the reaction pathway might involve in that case the η¹-propargylic intermediate **5c**.¹⁴ The latter would simply result from an S_N2-type substitution of the tosylate group by the anionic nucleophile [Ru₃(μ-Cl)(CO)₁₀][–] generated in situ (Scheme 4).

The X-ray crystal structure of **5b** is shown in Figure 2. The propargylic C10–Ru3 bond distance is ca. 2.28 Å: i.e., merely 13% longer than a pure covalent σ bond (theoretical distance *r*_{cov}(Ru) + *r*_{cov}(C) = 1.25 + 0.77 = 2.02 Å), revealing a strong σ-alkyl character of the complex.

(3) Comparative Theoretical Analysis of Allenyl Complexes **2b and **5b**.** To allow comparison of the related allenyl complex Ru₃(μ-Cl)(μ-η³-CH₃CCCH₂)(CO)₉ (**5b**) (stable) with the allenyl complex **2b** (elusive), the geometry of the latter was fully optimized at the B3PW91/6-31G* level (Figure 3). Indeed, let us remind the reader that, apart from Melikyan's report of a doubly [Co₂(CO)₆] complexed tris-propargylic cation,¹⁵ no X-ray diffraction data are available for standard [Co₂(CO)₆]–mono-propargylium complexes of type **1a**. The results indicate a similar geometry of the ligand in both the crystal structure of **5b** and the DFT-optimized structure

(13) Lavigne, G. Unpublished results.

(14) Cheng, M.-H.; Shu, H.-G.; Lee, G.-H.; Peng, S.-M.; Liu, R.-S. *Organometallics* **1993**, *12*, 108–115.

(15) Melikyan, G. G.; Bright, S.; Monroe, T.; Hardcastle, K. I.; Ciurash, J. *Angew. Chem., Int. Ed. Engl.* **1998**, *37*, 161–164.

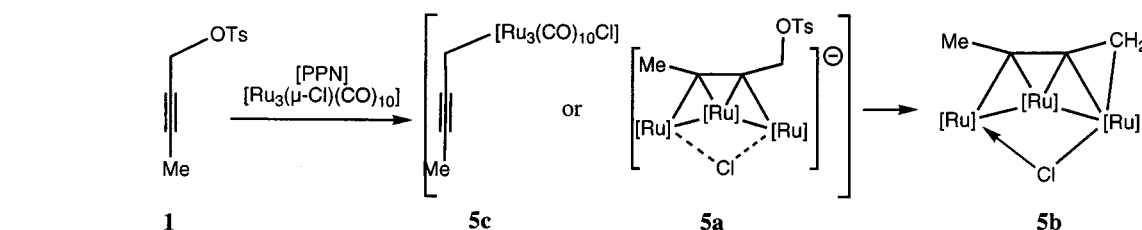
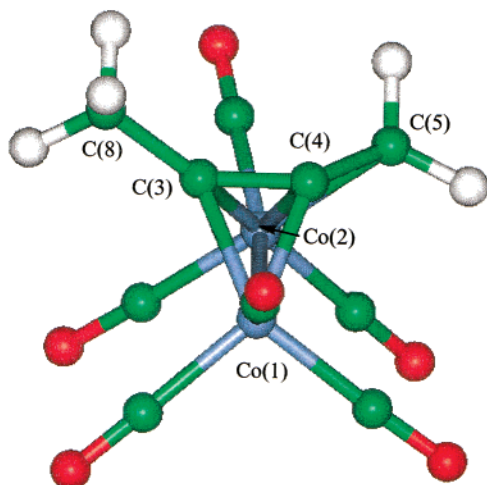
Scheme 4. Synthesis of the Allenyl Complex 5b through the Likely Intermediate 5c^{14 a}^a [Ru] = Ru(CO)₃.

Figure 3. Calculated structure of complex **2b** (B3PW91/6-31G*). Selected bond distances in Å: Co(1)–Co(2) = 2.470; C(3)–C(4) = 1.359; C(4)–C(5) = 1.388; Co(2)–C(5) = 2.142; C(3)–C(8) = 1.482. Selected bond angles in deg: C(3)–C(4)–C(5) = 134.6; C(4)–C(3)–C(8) = 134.0; H(6)–C(5)–H(7) = 115.2; C(4)–C(5)–H(6) = 119.9; C(4)–C(5)–H(7) = 120.1.

of **2b**. In particular, the shortest calculated Co...CH₂⁺ distance is 2.142 Å;¹⁶ i.e., 11% longer than the theoretical higher limit for an apolar pure σ bond, $r_{\text{cov}}(\text{Co}) + r_{\text{cov}}(\text{C}) = 1.16 + 0.77 = 1.93$ Å. It is thus as much of a bonding interaction as that measured for **5b** in the crystalline state. The distortions of the formal C(sp)–C(sp)–C(sp²) bond angle with respect to 180° in both **5b** (37.2°) and **2b** (45.4°) are found to be of the same magnitude, as well.

The electronic properties of **2b** and **5b** were further compared from calculations at the B3PW91/6-31G*/DZVP(M) level (M = Co, Ru), according to three criteria: frontier orbitals, atomic charges, and Fukui indices. In the following, heavy atoms of the allenyl complexes are denoted by the topological sequence: Me–C_γ–C_β–C_αH₂–[M_α]–[M_β]–[M_γ] for M = Ru only).

(i) Orbital Analysis. The frontier orbitals of **2b** and **5b** were analyzed, following a current procedure for the analysis of organometallic reactivity.¹⁷ The results tend to indicate a low reactivity of the propargylic C_α atom in both complexes: the LUMO (which is similar in shape to the corresponding HOMO) displays high p_{xy}- and d_{z²}-type contributions of the C_β and M_α centers, respectively, but no contribution of the propargylic C_α center (Figure 4). This rather unexpected feature is not an

Table 2. Mulliken Atomic Charges and Nucleophilic Fukui Indices for Complexes 2b and 5b^a

atom	Mulliken charges		Fukui indices		local softness	
	2b	5b	2b	5b	2b	5b
C _α	−0.34	−0.46	+0.007	0.00	+0.023	0.000
M _α	−0.95	−0.24	+0.128	+0.14	+0.456	+0.561
C _β	+0.13	−0.05	+0.047	+0.01	+0.169	+0.040
M _β	−0.79	−0.23	+0.047	+0.08	+0.168	+0.321
C _γ	+0.12	−0.12	+0.101	−0.02	+0.077	−0.080
M _γ		−0.23		+0.04		+0.160
CH ₃	−0.61	−0.53	−0.009	0.00	−0.030	0.000
Cl		−0.16		+0.03		+0.120

^a $f^{\text{N}}_{\text{Nb}}(A) = q_{\text{Nb}+1e}(A) - q_{\text{Nb}}(A)$, where Nb + 1e refers to the vertical one-electron reduction product of Nb. **2b** was calculated at the B3PW91/6-31G*/DZVP(Co) level, and **5b** was calculated at the B3PW91/6-31G*/DZVP(Ru) level.

Table 3. Energy Levels (in hartrees) of Frontier Orbitals Calculated at the 6-31G*/DZVP(Co, Ru) Level for Complexes 2b and 5b

MO	2b		5b	
	CH ₂ p _z weight	energy	CH ₂ p _z weight	energy
LUMO + 2	0	−0.2062	+	−0.0594
LUMO + 1	+	−0.2223	0	−0.0681
LUMO	0	−0.2639	0	−0.0781
HOMO	0	−0.4179	0	−0.2312

artifact of the DFT nature of the MO's. Indeed, semi-empirical ZINDO calculations afford the same qualitative results.¹⁸ For the primary propargylyum complex **2b**, these findings are apparently paradoxical with respect to EHMO calculations performed on a related Co₂(CO)₆-tertiary propargylyum complex;¹⁹ although the sum of bond angles around the propargylic C_αH₂ carbon atom is equal to 355.2°, and thus consistent with the classical view of sp² hybridization for C_α, the corresponding p_z AO is not found in the LUMO but in the LUMO + 1, which is 26.1 kcal mol^{−1} higher in energy (Table 3). For **5b**, the LUMO lies 116.6 kcal mol^{−1} higher than that of **2b**, suggesting that **5b** is globally less electrophilic than **2b**. In a similar way, however, the C_α p_z AO does not contribute to the LUMO of **5b**. It does not contribute to the LUMO + 1 either but exclusively to the LUMO + 2, lying 11.7 kcal mol^{−1} higher than the LUMO (Figure 4, Table 3).

It is also noteworthy that the significant contributions of C_β to the LUMO's of **2b** and **5b** are reminiscent of the well-established C_β regioselectivity of nucleophilic attack at η³-propargylic complexes of group 10 metals.²⁰

(16) In Melikyan's tetranuclear tris-propargylyum complex, the shortest measured Co...CH⁺ distance is equal to 2.81 Å.¹⁵

(17) See for example: Nelson, D. J.; Li, R.; Brammer, C. *J. Am. Chem. Soc.* **2001**, *123*, 1564–1568.

(18) ZINDO, 96.0/4.0.0; Molecular Simulation Inc., Cambridge, U.K., 1996.

(19) Gruselle, M.; El Hafa, H.; Nokolski, M.; Jaouen, G.; Vaissermann, J.; Li, L.; McGlinchey, M. *Organometallics* **1993**, *12*, 4917–4925.

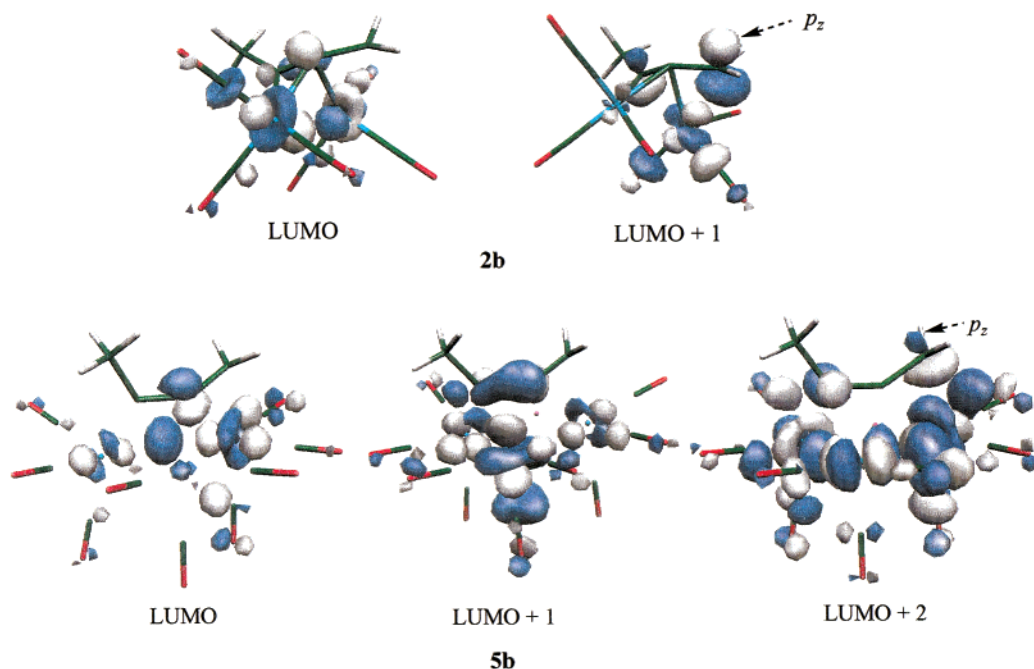


Figure 4. Lowest unoccupied MO's for allenyl complexes **2b** and **5b** at the B3PW91/6-31G*/DZVP(M) level (M = Co, Ru). The arrow indicates the formal p_z orbital of the sp^2 -hybridized propargylic CH_2 center.

(ii) Atomic Charges. A low reactivity of the propargylic C_α atom could also be anticipated from Mulliken population analysis (Table 2). Indeed, the atomic charges of the propargylic C_α and M_α (M = Co, Ru) centers are unexpectedly *negatively charged* in both the cationic complex **2b** and the neutral complex **5b**. Thus, the widely accepted "electrophilic" character of C_α in **2b** (Nicholas reaction) cannot be rationalized in terms of simple electronegativity arguments.

(iii) Fukui Indices. How do we conciliate the preceding theoretical analysis with Nicholas' experimental results? Reactivity is a two-partner property which depends not only on the relative electronegativity of the reactants ("plus likes minus" and conversely) but also on their relative softness ("hard likes hard" and "soft likes soft").²¹ In the HSAB theory, a molecule is fundamentally characterized by both its electronegativity (or chemical potential) and its softness, denoted as S . According to Pearson,²² $\eta = 1/S \approx I - A = E(M^{q+1}) + E(M^{q-1}) - 2[E(M^q)]$, where I and A are the vertical ionization potential and electron affinity and E is the molecular electronic energy. Its calculated value at the 6-31G*/DZVP(Co, Ru) level of theory shows that, as anticipated from qualitative considerations (charge, metal), **5b** is softer than **2b** ($S(2b) = 3.558 \text{ hartree}^{-1} < S(5b) = 4.008 \text{ hartree}^{-1}$). The difference is, however, rather small and does not a priori rule out the possibility of extending the reactivity of cationic cobalt complexes to the analogous neutral ruthenium complexes.

In the same manner as global electronegativity is determined by local (atomic) charges, global softness (S) can be split into local components: for a given molecule M^q , the *local softness* at the atom i is defined as: $S_i = f_i S$, where f_i is the Fukui index of the atom i for nucleophilic, electrophilic, or radical reactivity (see Computational Methods). This index is becoming a modern tool to compare the relative reactivity of sites within a given molecular complex.²³ Practically, the Fukui electrophilic reactivity index f_i^+ can be estimated by finite differences of Mulliken charges of atoms i in the one-electron-oxidized and -reduced structures. High positive values of f_i^+ indicate an enhanced reactivity of the atom i toward *soft nucleophiles*, while zero or negative values of f_i^+ indicate a specific reactivity toward *hard nucleophiles*.²⁴

f_i^+ indices were calculated at relevant atoms of **2b** and **5b** (Table 3). Their values are in accordance with Parr's theory: they roughly vary with the LUMO densities (Figure 4).^{21a} In particular, regarding soft nucleophiles, the less electrophilic allenyl carbon center in both of these complexes should definitely be C_γ and C_α . More precisely, the regioselectivity of soft nucleophiles can be ranked through local softness values:

cobalt series:

$$(S_{C_\alpha} = 0.023 \text{ hartree}^{-1}) C_\alpha < C_\gamma < C_\beta = \\ C_o_\beta < C_o_\alpha (S_{C_o_\alpha} = 0.456)$$

ruthenium series:

$$(S_{C_\gamma} = -0.080 \text{ hartree}^{-1}) C_\gamma < C_\alpha < C_\beta < Cl < \\ Ru_\gamma < Ru_\beta < Ru_\alpha (S_{Ru_\alpha} = 0.561 \text{ hartree}^{-1})$$

(20) (a) Tsuji, J.; Mandai, T., *Angew. Chem., Int. Ed. Engl.* **1995**, *34*, 2589–2612. (b) Chen, J.-T. *Coord. Chem. Rev.* **1999**, *190–192*, 1143–1168.

(21) (a) Parr, R. G.; Yang, W. *J. Am. Chem. Soc.* **1984**, *106*, 4049–4050. (b) Gazquez, J. L.; Mendez, F. *J. Phys. Chem.* **1994**, *98*, 4591–4593. (c) Li, Y.; Evans, J. N. S. *J. Am. Chem. Soc.* **1995**, *117*, 7756–7759. (d) Baekelandt, B. G.; Cedillo, A.; Parr, R. G. *J. Chem. Phys.* **1995**, *103*, 8548–8556. (e) De Proft, F.; Martin, J. M. L.; Geerlings, P. *Chem. Phys. Lett.* **1996**, *256*, 400–408.

(22) (a) Parr, R. G.; Pearson, R. G. *J. Am. Chem.* **1983**, *102*, 7512. (b) Pearson, R. G. *Inorg. Chem.* **1988**, *27*, 734–740.

(23) Chermette, H. *Coord. Chem. Rev.* **1998**, *178–180*, 699–721.

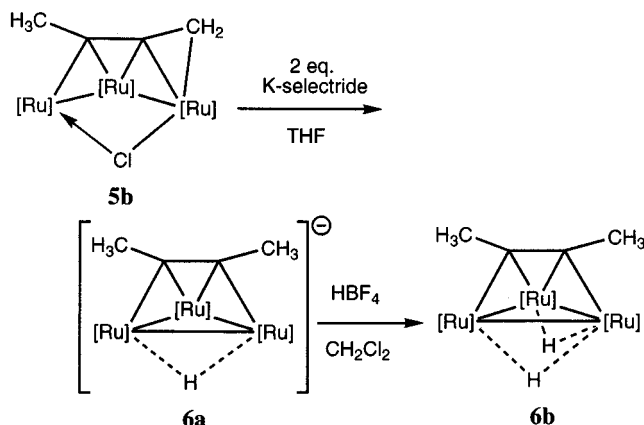
(24) Mendez, F.; Gazquez, J. L. *J. Am. Chem. Soc.* **1994**, *116*, 9298–9301.

Thus, the propargylic metal atom M_α is the most sensitive atom toward *soft nucleophiles*, whereas the propargylic carbon atoms C_α and C_γ are the most sensitive atoms toward *hard nucleophiles*. Moreover, the local softnesses of C_α and M_α are of the same order of magnitude in **2b** and **5b**. The Co–Ru analogy is therefore theoretically supported.

This analysis for the cobalt complex **2b** has, however, to be confronted with the well-documented experimental reactivity of cationic Nicholas-type complexes. The generally accepted mechanism of this reaction involves an exo attack of the propargylic carbon atom by the incoming nucleophile.^{7,25} It is then noteworthy that most of the nucleophiles reported to afford the C_α -substitution product are neutral (amines, alcohols, enol ethers, allyl silanes, ...). Considering that the few reported examples of anionic nucleophiles such as CH_3MgBr have not been thoroughly examined from a mechanistic point of view, the nature of the initial site of attack may be questioned.²⁶ Furthermore, anions are generally regarded as being softer than neutral species. Thus, according to the above theoretical results, neutral nucleophiles should be regarded as hard. On the other hand, these results suggest that initial attack by anionic nucleophiles should take place at the metal center.²⁷ A subsequent transfer to the organic ligand could, however, be envisaged. In the following experiments, a hydride was thus selected as a prototype of potentially transferable anionic nucleophile.

(4) Reaction of the Allenyl Ruthenium Complex 5b with a Hydride Donor. While the reactivity of cobalt complexes such as **2b** has been widely investigated, a preliminary exploration of the reactivity of **5b** was undertaken with K-Selectride as an efficient hydride carrier. The addition of 1 equiv of K-Selectride to the allenyl complex **5b** was found to result in the consumption of about 50% of the allenyl complex, as indicated by IR monitoring. Further addition of a second equivalent of K-Selectride afforded the anion $\text{K}[\text{Ru}_3(\mu\text{-H})(\mu\text{-MeCCMe})(\text{CO})_9]$ (**6a**) in quantitative spectroscopic yield (Scheme 5). As previously noted for complexes of the type $[\text{Ru}_3(\mu\text{-Cl})(\mu\text{-RCCR})(\text{CO})_9]^-$,^{9a,b} nucleophilic attack by a hydride takes place at the metal, resulting in a facile displacement of the halide. Here, the same substitution reaction takes place with concomitant transfer of the hydride from the metal to the carbon center (reductive elimination), thereby requiring 2 equiv of K-Selectride. Upon protonation of the anion **6a**, the neutral complex $\text{Ru}_3(\mu\text{-H})_2(\text{MeCCMe})(\text{CO})_9$ (**6b**) is recovered. The revealed electrophilic character of the metal core of **5b** is consistent with the above orbital and Fukui index analysis, which definitely points to the metal atoms as the softer electrophilic centers ($f^*(\text{Ru}_\alpha) = +0.14 > f^*(\text{Ru}_\beta) = +0.08 > f^*(\text{Ru}_\gamma) = +0.04$).

Scheme 5. Electrophilic Reactivity of the Allenyl Complex 5b



Bis-Propargylic Activation. Unlike substituted butatrienes, butatriene itself is unstable and undergoes radical polymerization, revealing a formal $\cdot\text{CH}_2\text{-C}\equiv\text{CCH}_2\cdot$ biradical character.²⁸ Nevertheless, butatriene has been long stabilized in *neutral* transition-metal complexes such as $\text{Fe}_2(\text{CO})_6(\text{C}_4\text{H}_4)$ and $\text{Fe}_2(\text{PPh}_3)(\text{CO})_5(\text{C}_4\text{H}_4)$.²⁹ Pushing the challenge further, stabilization of the corresponding $^+\text{CH}_2\text{C}\equiv\text{CCH}_2^+$ dication can be claimed to occur in dicationic complexes such as $[\text{Mo}_2\text{-Cp}_2(\text{CO})_4(\text{C}_4\text{H}_4)]^{2+}$,³⁰ $[\text{CoMoCp}(\text{CO})_5(\text{C}_4\text{H}_4)]^{2+}$,³¹ and $[\text{Co}_2(\text{CO})_2(\text{dppm})_2(\text{C}_4\text{H}_4)]^{2+}$.³² Nevertheless, although its existence is supported by a few examples of double Nicholas reactions,³³ the corresponding $[\text{Co}_2(\text{CO})_6(\text{C}_4\text{H}_4)]^{2+}$ complex has not been detected so far.³⁴ This quest would correspond to a double-propargylic activation of neutral 1,4-dihalo-³⁵ or 1,4-dioxybut-2-yne complexes **1a** into the *dicationic* limiting form **1d** (Scheme 6). The access to relevant species in the ruthenium series considered here would be facilitated, since it would correspond to the generation of the *monocationic* limiting form **IIId** (Scheme 6): namely, to a formal stabilization of the $\cdot\text{CH}_2\text{C}\equiv\text{CCH}_2^+$ monoradical cation. Let us mention that such a bonding situation of a substituted-butatriene fragment has been recently observed in neutral triruthenium carbonyl complexes bearing azavinylidene as an ancillary ligand.³⁶

(28) (a) Schubert, W. M.; Liddicoet, T. H.; Lanka, W. A. *J. Am. Chem. Soc.* **1954**, *76*, 1929–1932. (b) Morris, V. R.; Pollack, S. K. *J. Phys. Chem. B* **1998**, *102*, 5042–5046.

(29) (a) Nakamura, A.; Kim, P. J.; Hagihara, N. *J. Organomet. Chem.* **1965**, *3*, 7–15. (b) Joshi, K. K. *J. Chem. Soc. A* **1966**, 594–597. (c) Gerlach, J. N.; Wing, R. M.; Ellgen, P. C. *Inorg. Chem.* **1976**, *15*, 2959–2964. (c) Bruce, M. *Chem. Rev.* **1998**, *98*, 2832 and references therein.

(30) (a) Reutov, O. A.; Barinov, I. V.; Chertkov, V. A.; Sokolov, V. I. *J. Organomet. Chem.* **1985**, *297*, C25–C29. (b) McClain, M. D.; Hay, M. S.; Curtis, M. D.; Kampf, J. W. *Organometallics* **1994**, *13*, 4377–4386. $[\text{CoMoCp}(\text{CO})_5(\text{C}_4\text{H}_4)]^{2+}$.

(31) Gruselle, M.; Malezieux, B.; Vaissermann, J.; Amouri, H. *Organometallics* **1998**, *17*, 2337–2343.

(32) Bennett, S. C.; Phipps, M. A.; Went, M. J. *J. Chem. Soc., Chem. Commun.* **1994**, 225–226.

(33) (a) Gruselle, M.; Philomin, V.; Chaminant, F.; Jaouen, G.; Nicholas, K. M. *J. Organomet. Chem.* **1990**, *399*, 317. (b) Takano, S.; Sugihara, T.; Ogasawara, K. *Synlett* **1992**, 70–72.

(34) Green, J. R. *Chem. Commun.* **1998**, 1751–1752.

(35) The 1,4-dichlorobut-2-yne complex (**1a**, X = Cl) is known: Getini, G.; Gambino, O.; Rossetti, R.; Sappa, E. *J. Organomet. Chem.* **1967**, *8*, 149–154. The 1,4-diiodobut-2-yne complex (**1a**, X = I) is unknown, although it would be a stabilized form of 1,4-diiodo-2-butyne, which rapidly isomerizes to 2,3-diiodobutadiene: Wille, F.; Dirr, K.; Kerber, H. *Liebigs Ann. Chem.* **1955**, 591, 177.

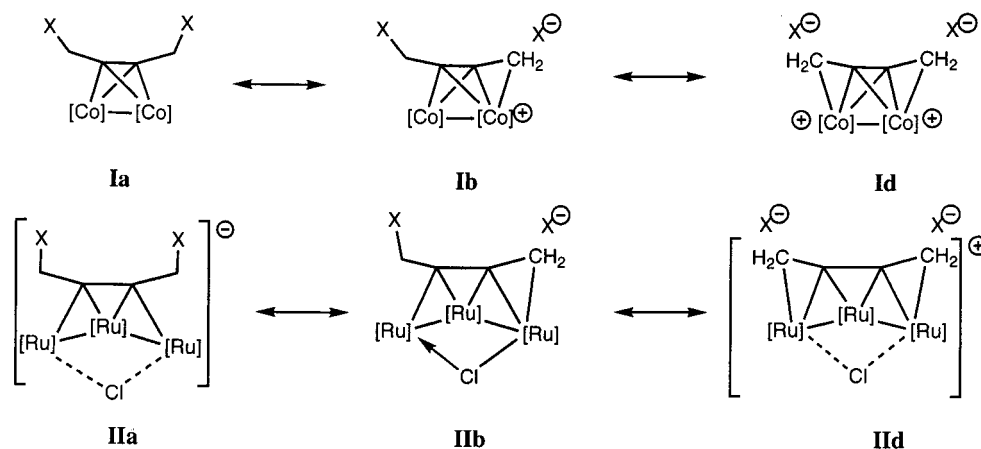
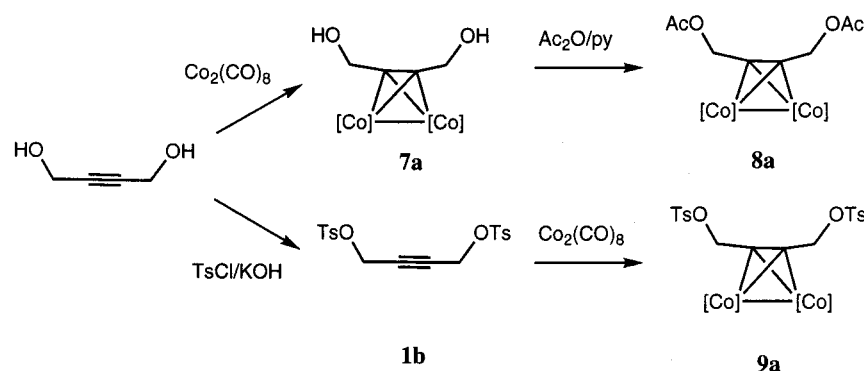
(36) Cabeza, J. A.; Grepioni, F.; Moreno, M.; Riera, V. *Organometallics* **2000**, *19*, 5424–5430.

(25) Schreiber, S. L.; Klimas, M. T.; Sammakia, T. *J. Am. Chem. Soc.* **1987**, *109*, 5749–5759.

(26) (a) Padmanabhan, S.; Nicholas, K. M. *J. Organomet. Chem.* **1981**, *212*, 115–124. (b), Soleilhavoup, M.; Chauvin, R. Unpublished results.

(27) Let us note that a NaBH_4 hydride is the sole anionic nucleophile reported to react with in situ formed Nicholas cobalt complexes such as **2b** to afford methyl products: Nicholas, K. M.; Siegel, J. *J. Am. Chem. Soc.* **1985**, *107*, 4999–5001. To be in accord with the present theoretical analysis, we could propose that a metal attack could occur first to give a $[\text{CoH}-\text{Co}-\text{CH}_2(\eta^2\text{-C}\equiv\text{CMe})]$ intermediate, which would then undergo reductive elimination.

Scheme 6. Possible Resonance Structures of Bis-Propargylic Cobalt and Ruthenium Complexes

Scheme 7. Preparation of Dioxy Bis-Propargylic Complexes^a^a [Co] = Co(CO)₃.

(1) Cobalt Series. The synthesis of the cobalt carbonyl complexes of but-2-yne-1,4-diol, its diacetic ester, and its ditosylyc esters, namely Co₂(CO)₆(μ-HOCH₂-C≡CCH₂OH) (**7a**), Co₂(CO)₆(μ-AcOCH₂C≡CCH₂OAc) (**8a**), and Co₂(CO)₆(μ-TsOCH₂C≡CCH₂OTs) (**9a**), was undertaken (Scheme 7).

The diacetox complex **8a** was isolated in 97% yield by acetylation of the previously known diol complex **7a**.^{31,37} Monocrystals of **8a** were analyzed by X-ray diffraction (Figure 5). The average C₂ symmetry of the solution structure revealed by NMR is preserved in the crystal state. It is similar to that of **7a**, which has been only recently reported.³¹ The η²-C≡C bond lengths in both **7a** and **8a** lie in the classical range (1.344 and 1.333 Å, respectively) and are thus much longer than in **3** (see preceding discussion). The C-C-CH₂ angle is 141.2(4)° in **8a** and 136.1° in **7a**, the latter value probably reflecting the occurrence of intramolecular O-H...H bonds.³¹ The Co...CH₂OAc distance is non-bonding, whereas the propargylic C-OAc bonds (1.446 and 1.438 Å) do not exhibit any lengthening with respect to standard values. No predissociation of the acetate group is therefore structurally observed.

Surprisingly, although the mono(tosyloxy)butyne complex **2a** was not observed (vide supra), reaction of the bis(tosyloxy)butyne **1b** with Co₂(CO)₈ in ether produced the heat-sensitive complex Co₂(μ-TsOCH₂C≡CCH₂OTs)(CO)₆ (**9a**) isolated in 88% yield. When a sample of **9a**

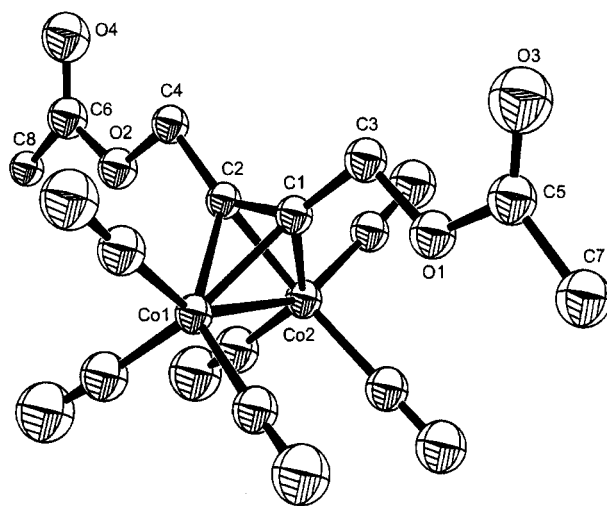
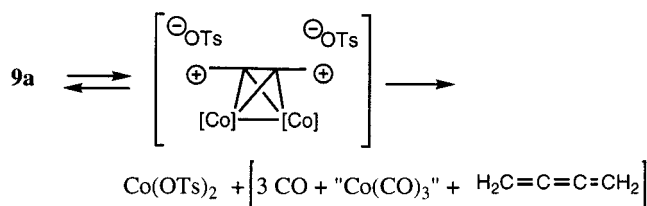
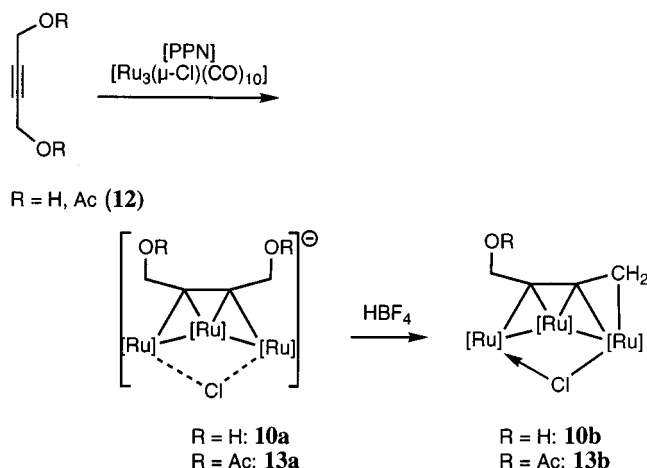


Figure 5. X-ray crystal structure of complex **8a**. Selected bond distances in Å: Co(1)–Co(2) = 2.4684(9); Co(1)–C(2) = 1.959(3); Co(1)–C(1) = 1.947(4); Co(2)–C(2) = 1.944(3); Co(2)–C(1) = 1.958(4); C(1)–C(2) = 1.333(5); O(1)–C(3) = 1.438(4); O(2)–C(4) = 1.446(5). Selected bond angles in deg: C(2)–C(1)–C(3) = 142.5(3); C(1)–C(2)–C(4) = 141.2(4); O(1)–C(3)–C(1) = 107.4(3); O(2)–C(4)–C(2) = 107.8(3).

was left in THF-*d*₈ solution at room temperature over several days, the propargylic CH₂ ¹³C and ¹H NMR signals disappeared, whereas the Co²⁺ complex [Co(H₂O)₆][OTs]₂ (identified by X-ray diffraction) was recovered.³⁸ This observation is consistent with an intramolecular reduction of the ligand by a cobalt(0)

(37) (a) Greenfield, H.; Friedel, R. A.; Wotiz, J.; Markby, R.; Wender, I. *J. Am. Chem. Soc.* **1954**, *76*, 1457–1458. (b) Pohl, D.; Ellermann, J.; Knoch, F. A.; Moll, M. *J. Organomet. Chem.* **1995**, *495*, C6–C11.

Scheme 8. Possible Oxidation of Cobalt by Its Dissociated 1,4-Bis(tosyloxy)but-2-yne Ligand^a
^a [Co] = Co(CO)₃.
Scheme 9. Stepwise Formation of a Neutral Allenyl Complex from But-2-yne-1,4-diol and 1,4-Diacetoxy-but-2-yne (12)^a
^a [Ru] = Ru(CO)₃.

atom and supports the picture **Id** of bis-propargylic activation (Schemes 6 and 8).

At 20 °C and 400 MHz, the ¹H NMR signals of the CH₂OTs moieties of **9a** in THF-*d*₈ show a specific shift with respect to the corresponding signals in DMF-*d*₇ (Δδ_H = 0.44 ppm). A similar solvent effect is observed for the corresponding 100 MHz ¹³C NMR signals (Δδ_{13C} = -6.45 ppm).³⁹ As previously established, NMR spectroscopy affords useful information on the dynamic behavior of propargylium dicobalt hexacarbonyl complexes.⁴⁰ Here, the observed dependence of chemical shifts on the solvent dielectric constant provides a hint that **9a** exists under the associated form (**1a**) in THF (ε = 7.52) but undergoes a solvent-induced polarization of the CH₂-OTs bond toward dissociated forms (**1b**, **1d**) in DMF (ε = 38.25).⁴¹

(2) Ruthenium Series. Reaction of the free butynediol HOCH₂C≡CCH₂OH with [PPN][Ru₃(μ-Cl)(CO)₁₀] resulted in the formation of the expected anionic cluster [PPN][Ru₃(μ-Cl)(μ-HOCH₂CCCH₂OH)(CO)₉] (**10a**) (IR monitoring). Protonation of **10a** with HBF₄ in THF afforded the hydroxyallenyl complex **10b**, analogous to the allenyl derivative **4b** (Scheme 9). The DCI/NH₃ MS spectrum of **10b** clearly revealed a parent ion multiplet at *m/z* 644, corresponding to a dehydroxylation of **10b**

occurring in the spectrometer and thereby generating the cationic butatriene complex **11d** (Scheme 6).

Likewise, the diacetoxybutyne **12** was allowed to react with [Ru₃(μ-Cl)(CO)₁₀]⁻ formed in situ from Ru₃(CO)₁₂ and [PPN][Cl]. The ruthenate complex [PPN][Ru₃(μ-Cl)(μ-AcOCH₂CCCH₂OAc)(CO)₉] (**13a**) was the sole carbonyl complex observed by IR. In contrast to the case of the mono(tosyloxy) ligand **1a**, the neutral acetate-allenyl complex Ru₃(μ-Cl)(μ-AcOCH₂CCCH₂)(CO)₉ (**13b**) was not spontaneously generated. Its formation required protonation with HBF₄ (Scheme 9). As in the case of the alcohol complex **10b**, the DCI/NH₃ MS spectrum of **13b** showed a parent ion multiplet at *m/z* 644, corresponding to the butatriene complex **11d** generated in the spectrometer via deacetoxylation of **13b** (Scheme 6).

Thus, the acetate substituents of **12** are not displaced by the [Ru₃(μ-Cl)(CO)₁₀]⁻ anion. In contrast, the tosylate substituents of **1b** were displaced by [Ru₃(μ-Cl)(CO)₁₀]⁻ to afford [PPN][OTs] and a novel type of ruthenium complex. The resulting IR spectrum exhibited an abnormal pattern, quite different from the one generally observed for ruthenates of the type [PPN][Ru₃(μ-Cl)(μ-RCCR)(CO)₉]. Nevertheless, according to IR monitoring, the reaction required 2 equiv of [PPN][Ru₃(μ-Cl)(CO)₁₀] for completion. Upon protonation, the newly generated elusive species produced **5b** in rather small yield along with roughly equal amounts of Ru₃(CO)₁₂ (Scheme 10). In accordance with related reactions of 1,4-bis(tosyloxy)but-2-yne (**1b**) with metalates [M]⁻ (M = FeCp(CO)₂,⁴² WCp(CO)₃)¹⁴), we propose that the initial interaction between **1b** and the cluster involves the methylene groups rather than the triple bond: the primary intermediate would thus correspond to the structure [M]-CH₂C≡CCH₂-[M] (**15c**),^{14,43} the bis-propargylic version of the mono-propargylic intermediate **5c**, proposed to result from the reaction of 1-(tosyloxy)but-2-yne (**1a**) with [Ru₃(μ-Cl)(CO)₁₀]⁻ (Scheme 4). In situ IR and NMR spectroscopy in THF-*d*₈, however, does not give evidence for the elusive species **15c**. Indeed, a detailed NMR analysis suggests that the primary intermediate finally evolves to the butatriene-type complex structure **15d**. As indicated by the two sets of ¹³C and ¹H CH₂ signals, and due to the stereogenicity of the triruthenium clusters, the product is actually a mixture of stereoisomers. In the ¹H NMR spectrum, two different propargylic CH₂ groups occur as pairs of doublets at high field (0.99, 1.94 for one isomer and 1.01, 1.93 ppm for the other) with a characteristic geminal coupling constant (²J_{HH} = 2.4 Hz for both the isomers). In the ¹³C spectrum the equivalent CH₂ groups of the two isomers occur at 43.74 and 43.82 ppm. ¹H-¹³C HMB and HMQC correlations assigned the central carbon atoms of the butatriene ligand at 128.83 and 131.17 ppm. Finally, a structure of the type **15d** might also be consistent with the observed behavior of the complex as a masked form of the alkyl ruthenium **15b**, giving the allenyl complex **5b** upon protonolysis of the propargylic C-Ru bond with HBF₄ (Scheme 10).

(38) Cabaleiro-Martínez, S.; Castro, J.; Romero, J.; García-Vázquez, J. A.; Sousa, A. *Acta Crystallogr., Sect. C* **2000**, C56, e249-e250.

(39) High fluxionality of the complex was also observed by VTP ¹H NMR in DMF-*d*₇ between -50 and 20 °C.

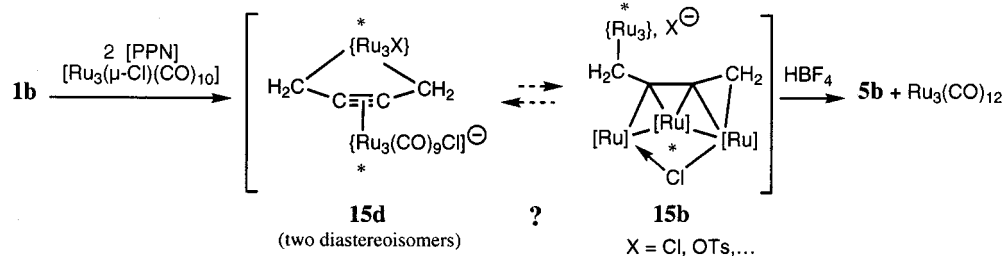
(40) Aime, S.; Milone, L.; Rossetti, R.; Stanghellini, P. L. *Inorg. Chim. Acta* **1977**, 22, 135-139.

(41) *CRC Handbook of Chemistry and Physics*, 78th ed.; Lide, D. R. Ed.; CRC Press: Boca Raton, FL, 1997; p 6-139.

(42) (a) Chiang, T.; Kerber, R. C.; Kimball, S. D.; Lauher, J. W. *Inorg. Chem.* **1979**, 18, 1687. (b) Rinze, P. V.; Müller, U. *Chem. Ber.* **1979**, 112, 1973.

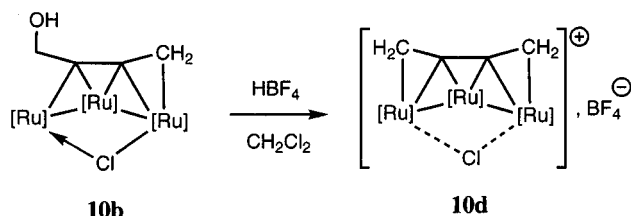
(43) This intermediate does not give the dissymmetrical structure **15b**, and this is consistent with the report that the triple bond of [M]-CH₂C≡CCH₂-[M] complexes does not displace the acetonitrile ligands of [Ru₃(CO)₁₀(MeCN)₂].¹⁴

Scheme 10. Reaction of 1,4-Bis(tosyloxy)but-2-yne (1b**) with 2 Equiv of in Situ Formed $[\text{PPN}][\text{Ru}_3(\mu\text{-Cl})(\text{CO})_{10}]^a$**



^a $[\text{Ru}] = \text{Ru}(\text{CO})_3$. It might be proposed that $\{\text{Ru}_3\} = [\text{Ru}_3\text{Cl}(\text{CO})_{10}]$.

Scheme 11. Formation of a Cationic Butatriene Ruthenium Complex^a



^a $[\text{Ru}] = \text{Ru}(\text{CO})_3$.

The above results were indicative that good leaving groups such as tosylates are not exploitable in the context of bis-propargylic activation. This led us to devise an alternate strategy to generate the butatriene complex **10d**, keeping in mind the observation of its characteristic pattern in the mass spectrum of the hydroxyallenyl complex **10b**. Accordingly, **10b** was treated with 1 equiv of HBF_4 in dichloromethane, leading to a new cationic species which was crystallized from the same solvent.⁴⁴ The absence of a hydride signal clearly indicated that protonation does not take place at the metal core, whereas the IR spectrum exhibited high-frequency $\text{C}\equiv\text{O}$ absorptions, consistent with the occurrence of a cationic complex. The complex was formulated as the cationic species $[\text{Ru}_3(\mu\text{-Cl})(\mu\text{-CH}_2\text{-CCCH}_2)(\text{CO})_9]^+$ (**10d**) on the basis of NMR and mass spectrometry. It was isolated in 54% yield (Scheme 11).

This complex is stable in CD_3CN or $(\text{CD}_3)_2\text{CO}$ solutions at low temperature, allowing for its characterization by ^1H and ^{13}C NMR. In the ^1H NMR spectrum, two doublets of doublets occur at 4.48 and 5.06 ppm. Their large ($^2J_{\text{HH}} = 3.9$ Hz) and small ($^5J_{\text{HH}} = 2.8$ Hz) coupling constants are consistent with two geminal $\text{C}_{\text{sp}^2}\text{-H}$ protons of a butatriene ligand in a C_s environment (owing to the C_s symmetry of the $\text{Ru}_3(\mu\text{-Cl})(\text{CO})_9$ core, a static C_2 symmetry can be ruled out). The C_s symmetry is also supported by the observation of five IR absorption bands, consistent with the $3 A' + 2 A''$ stretching vibration analysis for this symmetry group. The butatriene picture of the ligand is validated by the coupling constant $^1J_{\text{CH}} = 164$ Hz, which is characteristic for sp^2 carbon atoms. Finally, the $^2J_{\text{HH}}$ and $\delta^{13}\text{C}$ ($= 43.00$ ppm) values of the CH_2 groups are almost identical with those observed in situ for **15d** (see above), giving further support to the occurrence of a butatriene unit in the latter.

(44) A side product remained soluble in CH_2Cl_2 , but its exact structure could not be determined: see Experimental Section.

Conclusion

The present work shows that the reactivity of functionalized alkynes toward cobalt and ruthenium clusters is dramatically affected by the nature of the leaving group occupying one or two propargylic positions. Whenever an OH or OAc substituent is present in propargylic position(s), the initial interaction between the alkyne and the cluster involves "normal" coordination of the triple bond. Further elimination of the leaving group and activation of a propargylic position then requires the assistance of an acid. In contrast, an "abnormal" behavior is observed in the presence of a very good leaving group such as tosylate, particularly in the case of 1,4-bis(tosyloxy)but-2-yne (**1b**), where putative **1d** and elusive **15d** butatriene-type complexes are suggested to be produced in situ. A comparison of the orbitals and Fukui indices for the elusive (DFT-optimized) allenyl cobalt complex $[\text{Co}_2(\mu\text{-}\eta^2\text{-RCCCH}_2)(\text{CO})_6]^+$ (**2b**) and the isolated allenyl ruthenium complex $\text{Ru}_3(\mu\text{-Cl})(\mu\text{-}\eta^3\text{-CH}_3\text{-CCCH}_2)(\text{CO})_9$ (**5b**) allows us to anticipate a parallel electrophilic behavior for these two complexes. Finally, the above experimental and theoretical results support a structural analogy between cobalt and ruthenium alkyne clusters, possibly exploitable in terms of reactivity. Significantly, the low Mulliken charge of the chloride ligand and the high-lying LUMO make the allenyl ruthenium complex **5b** globally less electrophilic than the allenyl cobalt complex **2b**. A Fukui index analysis provides a rationale for the specific Nicholas propargylic reactivity of allenylcobalt complexes with neutral nucleophiles: within the framework of the HSAB theory, those have to be considered as *hard*, while anionic nucleophiles have to be considered as *soft* and should react at the cobalt carbonyl center. Such an analysis indicates the same trend in the ruthenium series. A hydride was indeed shown to react at the metal center of the neutral complex **5b**, as predicted for soft nucleophiles. The reactivity of hard neutral nucleophiles should be, however, restored by the cationic charge of the butatriene complex $[\text{Ru}_3(\mu\text{-Cl})(\mu\text{-CH}_2\text{CCCH}_2)(\text{CO})_9]^+$ (**10d**). The latter is easily prepared in two steps from the commercially available but-2-yne-1,4-diol. Systematic studies of the nucleophilic C-functionalization of the butatriene ligand of **10d** will thus be the next challenge, with the ultimate goal of synthesizing carbomeric carbocycles by alcyne-propargyl coupling.⁵¹

Experimental Section

THF and ether were distilled over Na/benzophenone. Pentane and dichloromethane were distilled over P_2O_5 . $\text{Ru}_3(\text{CO})_{12}$

was prepared from $\text{RuCl}_3 \cdot 3\text{H}_2\text{O}$ (Johnson-Matthey) according to a recently improved procedure.⁴⁵ $\text{Co}_2(\text{CO})_8$ was purchased from Strem Chemicals. 2-Butyn-1-ol, 2-butyne-1,4-diol, tosyl chloride, and acetic anhydride were purchased from Fluka. Elemental analyses were performed at the Service de Microanalyse du LCC on a Perkin-Elmer 2400 apparatus. IR spectra were recorded on a Perkin-Elmer GX FT-IR spectrometer using a CaF_2 cell. 1D-NMR spectra were recorded on Bruker AC 200 and AM 250 spectrometers, at 200 and 250 MHz, respectively, for ^1H and at 50 and 63 MHz, respectively, for ^{13}C . 2D-NMR spectra were recorded on a Bruker AMX 400 apparatus. Positive chemical shifts at low field are expressed in ppm by reference to TMS.

Preparation of 1-(Tosyloxy)but-2-yne (1a).⁴⁶ Tosyl chloride (2.94 g, 15.4 mmol) was added to a solution of but-2-yn-1-ol (0.939 g, 13.4 mmol) in acetonitrile (5 mL). After it was stirred for 10 min at room temperature, the mixture was cooled to 0 °C and 10 M aqueous KOH solution (3 mL) was added. After it was stirred overnight at room temperature, the mixture was extracted in Et_2O (3 \times 30 mL). The organic phase was dried over Na_2SO_4 , filtered, and dried under vacuum. The resulting solid **1a** was recrystallized from methanol and recovered as white crystals (1.42 g, 47%). Mp: 49–50 °C. ^1H NMR (CDCl_3): δ 1.71 (t, 3 H, $\text{CH}_3\text{C}\equiv$); 2.43 (s, 3 H, $\text{CH}_3\text{C}_6\text{H}_4$); 4.65 (s, 2 H, $\equiv\text{CCH}_2\text{O}$); 7.33 (d, 2 H, $^3J_{\text{HH}} = 8.1$ Hz, *o*-CH); 7.80 (d, 2 H, $^3J_{\text{HH}} = 8.1$ Hz, *m*-CH). $^{13}\text{C}\{^1\text{H}\}$ NMR (CDCl_3): δ 3.60 ($\text{CH}_3\text{C}\equiv$); 21.66 ($\text{CH}_3\text{C}_6\text{H}_4$); 58.70 ($\equiv\text{CCH}_2\text{O}$); 71.00 ($\text{MeC}\equiv$); 86.18 ($\text{MeC}\equiv\text{O}$); 128.13, 129.72 (*o*- and *m*-CH); 133.26 (*ipso*-CMe); 144.88 (*ipso*- CSO_3). MS (DCI/ NH_3): m/z 259 ($[\text{M} + \text{NH}_4]^+$), 242 ($[\text{M} + \text{H}]^+$). IR (Et_2O): ν 942 (s), 1096 (w), 1178 (s), 1190 (m), 1369 (m), 1599 (w), 2924 (w) cm^{-1} . Anal. Found (calcd): C, 58.89 (58.92); H, 5.40 (5.58); S, 14.53 (14.27).

Preparation of 1,4-Bis(tosyloxy)but-2-yne (1b).⁴⁶ The above procedure was applied to the present synthesis, from tosyl chloride (30.6 g, 160.3 mmol) and 2-butyne-1,4-diol (6.00 g, 69.7 mmol) as reagents. Recrystallization from methanol afforded **1b** as white crystals (11.52 g, 47%). ^1H NMR (CDCl_3): δ 2.44 (s, 6 H, $\text{CH}_3\text{C}_6\text{H}_4$); 4.56 (s, 4 H, $\equiv\text{CCH}_2\text{O}$); 7.33 (d, 4 H, $^3J_{\text{HH}} = 8.4$ Hz, *o*-CH); 7.55 (d, 4 H, $^3J_{\text{HH}} = 8.4$ Hz, *m*-CH). ^{13}C NMR (CDCl_3): δ 21.84 (q, $^1J_{\text{CH}} = 127.3$ Hz, $\text{CH}_3\text{C}_6\text{H}_4$); 57.25 (t, $^1J_{\text{CH}} = 155.4$ Hz, $\equiv\text{CCH}_2\text{O}$); 81.08 (s, $\text{MeC}\equiv$); 86.18 ($\text{MeC}\equiv\text{O}$); 128.24, 130.07 (2 d, $^1J_{\text{CH}} = 165.0$ Hz, *o*- and *m*-CH); 132.86 (s, *ipso*-CMe); 145.61 (s, *ipso*- CSO_3). IR (CD_2Cl_2): ν 1095 (w), 1178 (s), 1191 (s), 1360 (w), 1372 (vs), 1445 (w), 1495 (w), 1598 (m) cm^{-1} . Anal. Found (calcd): C, 54.43 (54.81); H, 4.40 (4.60).

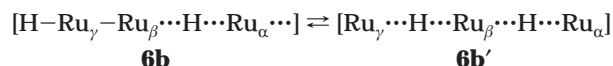
Preparation of 1,4-Diacetoxybut-2-yne (12). Pyridine (5 mL, 62 mmol) was syringed into a solution of but-2-yne-1,4-diol (1.291 g, 0.15 mmol) in acetic anhydride (15 mL, 159 mmol). After the mixture was stirred for 3 h at room temperature, 1 M aqueous HCl (50 mL) was added. The mixture was extracted in Et_2O (2 \times 20 mL). The organic phase was dried over MgSO_4 , filtered, concentrated, and dried overnight under vacuum. Pure diacetate **12** was obtained as a colorless oil (1.140 g, 45%). ^1H NMR (CDCl_3): δ 2.02 (s, 6 H, CH_3CO); 4.64 (s, 4 H, $\equiv\text{CCH}_2\text{OAc}$). ^{13}C NMR (CDCl_3): δ 20.70 (q, $^1J_{\text{CH}} = 129.9$ Hz, CH_3CO); 52.09 (t, $^1J_{\text{CH}} = 152.9$ Hz, $\equiv\text{CCH}_2\text{O}$); 80.77 (s, $\text{C}\equiv\text{C}$); 1170.11 ($-\text{C}=\text{O}$). IR (CDCl_3): ν 1028 (s), 1158 (m), 1224 (vs), 1360 (w), 1379 (m), 1434 (w), 1449 (w), 1745 (vs), 2947 (w) cm^{-1} . Anal. Found (calcd): C, 56.28 (56.47); H, 6.11 (5.92).

Preparation of Complex 3. Dicobalt octacarbonyl (0.916 g, 2.7 mmol) was added to a solution of 1-(tosyloxy)but-2-yne

(**1a**; 0.60 g, 2.7 mmol) in Et_2O (50 mL) at room temperature. The reaction was monitored by IR spectroscopy: after 3 h of stirring, the bridging carbonyl band at 1846 cm^{-1} disappeared, and the solution was evaporated to dryness. The solid was dissolved in pentane and filtered through Celite. The filtrate was then evaporated, giving **3** as a red oil (0.736 g, 79%). ^1H NMR (CDCl_3): δ 2.65 (s, 6 H, $\text{CH}_3\text{C}\equiv$); 4.82 (s, 4 H, CH_2O). ^{13}C NMR (CDCl_3): δ 20.26 (q, $^1J_{\text{CH}} = 130.2$ Hz, $\text{CH}_3\text{C}\equiv$); 71.63 (t, $^1J_{\text{CH}} = 144.7$ Hz, CH_2O); 92.35, 93.25, (2 s, $\eta^2\text{-C}\equiv\text{C}$); 199.67 (s, $\text{Co}_2(\text{CO})_6$). MS (DCI/ NH_3): m/z 712 ($[\text{M} + \text{NH}_4]^+$). IR (pentane): $\nu_{\text{C}=\text{O}}$ 2093 (m), 2057 (s), 2029 (s) cm^{-1} . Recrystallization from methanol afforded red crystals suitable for an X-ray structure determination.

Preparation of Complex 5b. $\text{Ru}_3(\text{CO})_{12}$ (0.300 g, 0.47 mmol) and $[\text{PPN}][\text{Cl}]$ (0.270 g, 0.47 mmol) were dissolved in THF (30 mL). The solution was stirred for 3 h at room temperature under N_2 bubbling via a needle in the solution. The formation of $[\text{PPN}][\text{Ru}_3(\mu\text{-Cl})(\text{CO})_{10}]$ was monitored by IR (in THF, $\nu_{\text{C}=\text{O}}$ 2070 (w), 2026 (s), 1994 (vs), 1981 (s), 1952 (s), 1908 (w), 1801 (m), 1775 (w) cm^{-1}). 1-(Tosyloxy)but-2-yne (**1a**; 0.106 g, 0.47 mmol) was added. After a few minutes a white solid ($[\text{PPN}][\text{OTs}]$) precipitated. The solution was filtered and evaporated to dryness. The brown residue was then dissolved in a few drops of dichloromethane and flash-chromatographed over silica gel (1/1 pentane/ CH_2Cl_2). After evaporation, complex **5b** was obtained as a brown solid (0.208 g, 68%). ^1H NMR (CD_2Cl_2): δ 3.07 (s, 3 H, CH_3); 3.59 (d, $^2J_{\text{HH}} = 3.2$ Hz, 1 H, CHHRu); 4.62 (d, $^2J_{\text{HH}} = 3.2$ Hz, 1 H, CHHRu). ^{13}C NMR (CD_2Cl_2): δ 34.09 (t, $^1J_{\text{CH}} = 165.0$ Hz, CH_2Ru); 37.29 (q, $^1J_{\text{CH}} = 129.1$ Hz, CH_3); 148.70 (s, RuCCH_2Ru); 186.00, 189.08, 190.76, 191.99, 194.83, 196.18, 196.88 (br), 197.44, 199.47 (9 s, $\text{Ru}_3(\text{C}\equiv\text{O})_9$); 213.06 (pseudo q, $^2J_{\text{CH}} = 5.1$ Hz, MeCRu). MS (DCI/ NH_3): m/z 646 ($[\text{M} + \text{H}]^+$). IR (THF): $\nu_{\text{C}=\text{O}}$ 2099 (m), 2076 (s), 2061 (w), 2047 (vs), 2038 (m), 2020 (m), 2015 (m), 1997 (m), 1983 (w). Anal. Found (calcd): C, 24.27 (24.25); H, 0.71 (0.78); Cl, 5.42 (5.51). The solid was recrystallized from CH_2Cl_2 /pentane to afford yellow crystals suitable for an X-ray structure determination.

Preparation of Complexes 6a and 6b. A 1 M solution of K-Selectride in THF (0.155 mL, 0.155 mmol) was syringed into a solution of the allenyl complex **5b** (0.100 g, 0.155 mmol) in THF (10 mL) at room temperature. The solution turned deep red, while IR monitoring indicated that only half of the allenyl complex had been consumed. Another 1 equiv of the K-Selectride solution (0.155 mL, 0.155 mmol) was added, and the final IR spectrum was fully consistent with the complex $[\text{K}][\text{Ru}_3(\mu\text{-H})(\text{CO})_9(\text{MeCCMe})]$ (**6a**). The solution was evaporated to dryness, and the residue was dissolved in CH_2Cl_2 (10 mL). The solvent was then cooled to -78 °C, and $\text{HBF}_4 \cdot \text{OEt}_2$ (0.021 mL, 0.154 mmol) was syringed in. The latter was concentrated and then chromatographed over silica gel (1/1 pentane/dichloromethane). After evaporation, complex **6b** was obtained as a brown solid (0.045 g, 47%). IR (CH_2Cl_2): $\nu_{\text{C}=\text{O}}$ 2017 (m), 1987 (vs), 1968 (broad s), 1944 (broad m) cm^{-1} . MS (DCI/ NH_3): m/z 614 ($[\text{MH}]^+$); 586 ($[\text{MH} - \text{CO}]^+$). ^1H NMR (CDCl_3): δ -20.87 , -18.65 , -17.80 (3 s, 2 H; $\text{Ru}\cdots\text{H}\cdots\text{Ru}$); 2.61 (s, 6H, $\text{C}_2(\text{CH}_3)_2$). Unless some decomposition occurs in CDCl_3 , the occurrence of three hydride signals could be interpreted as a result of a slow interconversion between tautomeric species **6b** (two types of different hydrides) and **6b'** (one type of equivalent hydrides):



Preparation of Complex 7a. But-2-yne-1,4-diol (1.00 g, 1.16 mmol) was dissolved in diethyl ether (60 mL) at 40 °C. $\text{Co}_2(\text{CO})_8$ (3.97 g, 1.16 mmol) was added, and the mixture was stirred for 3 h. The solution was concentrated twice, and pentane (50 mL) was added. The solution was cooled to 0 °C for ca. 20 min and then filtered. The remaining brown solid

(45) (a) Lavigne, G.; Saccavini, C.; Chauvin, R. In *Inorganic Experiments*, 2nd ed.; Woolins, D. J., Ed.; VCH: Weinheim, Germany, in press. (b) Faure, M.; Maurette, L.; Donnadieu, B.; Lavigne, G. *Angew. Chem., Int. Ed. Engl.* **1999**, 38, 518–522.

(46) Eglinton, G.; Whiting, C. *J. Chem. Soc.* **1950**, 3650–3653. For other uses of this substrate, see: Brouard, C.; Pornet, J.; Miginiac, L. *Synth. Commun.* **1994**, 24(21), 3047. Bertram, H. J.; Jansen, M.; Peters, K.; Meier, A.; Winterfeldt, E. *Liebigs Ann. Chem.* **1986**, 456. De Meijere, A.; Jaekel, F.; Simoa, A.; Borrmann, H.; Köhler, J.; Johnels, D.; Scott, L. T. *J. Am. Chem. Soc.* **1991**, 113, 3995.

was redissolved in diethyl ether, and this solution was filtered over a small pad of Celite. The filtrate was concentrated to dryness, and **7a** was obtained as a red microcrystalline solid (2.25 g, 6.05 mmol, 52%). Mp: 130–134 °C. IR (Et₂O): $\nu_{\text{C}\equiv\text{O}}$ 2093 (m), 2053 (s), 2029 (s) cm⁻¹. ¹H NMR (CDCl₃): δ 2.61 (s, 2 H, OH); 4.86 (s, 4 H, CH₂).

Preparation of Complex 8a. Butynediol complex **7a** (0.80 g, 2.15 mmol) was dissolved in Ac₂O (5 mL) at room temperature. Pyridine was added (0.870 mL, 10.75 mmol) and the solution was stirred for 12 h. One molar aqueous HCl (20 mL) was added, and the mixture was extracted in Et₂O. The organic phase was washed with 5% aqueous NaHCO₃ and dried over MgSO₄. Complex **8a** was obtained as a microcrystalline solid (0.949 g, 97%). MS (DCI/NH₃): m/z 474 ([M + NH₄]⁺); 397 ([M - CH₃CO₂ + H]⁺), 369 ([M - CH₃CO₂ - CO + H]⁺), 341 ([M - CH₃CO₂ - 2 CO + H]⁺). IR (CDCl₃): $\nu_{\text{C}\equiv\text{O}}$ 2099 (m), 2061 (s), 2036 (s), 1740 (m) cm⁻¹. ¹H NMR (CDCl₃): δ 2.10 (s, 6 H, CH₃); 5.24 (s, 4 H, CH₂). ¹³C{¹H} NMR (CDCl₃): δ 20.28 (s, CH₃); 64.12 (s, CH₂O), 89.20 (s, C \equiv C), 170.40 (s, MeC=O), 198.44 (s broad, Co₂(CO)₆).

The solid could be recrystallized from methanol (0.621 g, 63%) to afford single crystals suitable for an X-ray structure determination. Anal. Found (calcd): C, 37.11 (36.97); H, 2.10 (2.21); Co, 24.31 (25.84).

Preparation of Complex 9a. Co₂(CO)₈ (0.87 g, 2.5 mmol) was added to a suspension of 1,4-bis(tosyloxy)but-2-yne (**1b**; 1.00 g, 2.5 mmol) in Et₂O (50 mL). The dark brown color of the solution faded off, while a red solid precipitated over 3 h of stirring at room temperature. The solution was concentrated twice and then filtered. Complex **9a** was obtained as a brown solid (1.50 g, 2.2 mmol, 88%). ¹H NMR (THF-*d*₆): δ 2.46 (s, 6 H, CH₃); 5.23 (s, 4 H, CH₂); 7.45 and 7.85 (2 d, ³J_{HH} = 8.0 Hz, aromatic CH). ¹³C{¹H} NMR (THF-*d*₆): δ 20.09 (CH₃), 70.71 (CH₂), 88.32 (η^2 -C \equiv C), 128.19 and 130.18 (*o* and *m* aromatic CH), 134.07 (aromatic CSO₃), 145.34 (aromatic CMe), 198.57 (broad, Co₂(CO)₈). ¹H NMR (400 MHz, DMF-*d*₇, 293 K): δ 2.41 (s, 6 H, CH₃); 5.67 (s, 4 H, CH₂); 7.30 and 7.56 (2 d, ³J_{HH} = 8.0 Hz, aromatic CH). High fluxionality of the complex was observed by VTP ¹H NMR in DMF-*d*₇ between -50 and 20 °C. ¹³C{¹H} NMR (100 MHz, DMF-*d*₇, 293 K): δ 20.78 (CH₃), 64.26 (CH₂), 90.87 (s, η^2 -C \equiv C), 127.70 and 129.42 (*o* and *m* aromatic CH and aromatic CMe), 139.55 (aromatic CSO₃), 200.00 (broad, Co₂(CO)₆). (-)-ESMS: m/z 171 (TsO⁻) (no signal from (+)-ESMS or DCI/NH₃). IR (THF): $\nu_{\text{C}\equiv\text{O}}$ 2102 (vs), 2064 (vs), 2039 (vs); $\nu_{\text{S}(\text{O})_2}$ 1364 (s); 1189 (s), 1179 (s) cm⁻¹. IR (KBr): $\nu_{\text{C}\equiv\text{O}}$ 2103 (w), 2117 (vs), 2063 (vs), 2031 (vs); $\nu_{\text{S}(\text{O})_2}$ 1348 (w); 1188 (m), 1171 (m) cm⁻¹. UV-vis: λ_{abs} 276 (ϵ_{max}); 310 (sh); 352 nm ($\epsilon/\epsilon_{\text{max}}$ = 0.41).

Several attempts to obtain elemental analyses gave erratic results: this is likely due to the poor stability of the complex, the purity of which is however supported by ¹H and ¹³C{¹H} NMR spectra (Supporting Information).

Preparation of Complexes 10a and 10b. Ru₃(CO)₁₂ (0.200 g, 0.313 mmol) and [PPN][Cl] (0.180 g, 0.314 mmol) were dissolved in THF (20 mL). The solution was stirred for 3 h at room temperature under N₂ bubbling via a needle in the solution. The formation of [PPN][Ru₃(μ -Cl)(CO)₁₀] was monitored by IR. 1,4-Dihydroxybut-2-yne (0.027 g, 0.314 mmol) was added, and after a few minutes the solution turned deep brown. Complex **10a** was obtained after evaporation of the solvent (0.402 g, quantitative). IR (THF): $\nu_{\text{C}\equiv\text{O}}$ 2071 (w), 2059 (w), 2033 (s), 1989 (vs), 1978 (s), 1958 (m), 1947 (m), 1919 (w), 1835 (vw), 1681 (vw), 1589 (vw).

The solution was then cooled to -20 °C, and HBF₄·OEt₂ (0.043 mL, 0.316 mmol) was syringed in. The reaction medium was filtered and the solvent was removed under vacuum, leaving a crude material (0.282 g) which was extracted with diethyl ether (20 mL). Evaporation of the solvent yielded complex **10b** (0.148 g, 70% crude yield). Although the unfunctional allenyl complex **5b** could be purified further by chromatography, chromatography of crude **10b** over silica gel or

alumina was avoided due to a partial decomposition of the complex on the column. Nevertheless, the residual PPN⁺ salt could be removed by a second extraction in pentane (2 × 20 mL) and subsequent evaporation, which afforded complex **10b** associated with ca. 10% of pentane as indicated by the ¹H NMR spectrum (Supporting Information) (yield 0.042 g, 20%). IR (THF): $\nu_{\text{C}\equiv\text{O}}$ 2099 (w), 2074 (s), 2044 (vs), 2005 (s), 1982 (sh, w), 1964 (sh, w), 1589 (vw) cm⁻¹. ¹H NMR (CDCl₃): δ 2.28 (t, ³J_{HH} = 5.2 Hz, 2H; OH); 3.61 and 4.63 (2 d, ²J_{HH} = 3.3 Hz, CH₂Ru); 4.90 and 5.09 (2 dd, ³J_{HH} = 5.2 Hz, ²J_{HH} = 13.6 Hz; CH₂O). ¹³C{¹H} NMR (CDCl₃): δ 35.19 (CH₂Ru); 73.90 (CH₂O); 152.46 (RuCCH₂Ru); 185.50, 188.61, 191.42, 193.29, 195.36, 196.23 (br), 196.75, 198.99 (8 s, Ru₃(C \equiv O)₉); 209.42 (OCH₂CRu). MS (DCI/NH₃): m/z 679 ([M + NH₄]⁺); 661 ([M + NH₄ - H₂O]⁺); 644 ([MH - H₂O]⁺). Anal. Found (calcd) for **10b**·0.1 (pentane): C, 24.60 (24.38); H, 0.71 (0.96).

Preparation of Complexes 13a and 13b. Ru₃(CO)₁₂ (0.300 g, 0.47 mmol) and [PPN][Cl] (0.270 g, 0.47 mmol) were dissolved in THF (30 mL). The solution was stirred for 3 h at room temperature under an N₂ stream. The formation of [PPN]-[Ru₃(μ -Cl)(CO)₁₀] was monitored by IR. A solution of 1,4-diacetoxybut-2-yne (0.080 g, 0.47 mmol) in THF (10 mL) was added. After a few minutes the solution turned brown. Complex **13a** was characterized by IR. IR (THF): $\nu_{\text{C}\equiv\text{O}}$ 2061 (w), 2036 (s), 1992 (vs), 1981 (s), 1962 (m), 1952 (m), 1924 (w), 1835 (vw), 1736 (m), 1589 (vw) cm⁻¹.

The solution was then cooled to -20 °C, and HBF₄·OEt₂ (0.064 mL, 0.47 mmol) was added dropwise. The solution was filtered and then evaporated to dryness under vacuum. The crude material (0.478 g) was obtained and then extracted with diethyl ether (2 × 20 mL). Evaporation of the solvent yielded complex **13b** (0.215 g, 65% crude yield). Residual PPN⁺ salt was removed by a second extraction with pentane (2 × 20 mL) followed by evaporation, affording pure complex **13b** (0.076 g, 23%). ¹H NMR (CDCl₃): δ 3.59, 4.51 (2 d, ²J_{HH} = 3.3 Hz, 2 H, CH₂Ru); 5.05 and 5.53 (2 d, ²J_{HH} = 13.6 Hz, CH₂OAc). ¹³C NMR (CDCl₃): δ 20.84 (q, ¹J_{CH} = 129.8 Hz, CH₃CO); 38.74 (t, ¹J_{CH} = 165.6 Hz, CH₂Ru); 74.73 (t, ¹J_{CH} = 149.6 Hz, CH₂OAc); 144.60 (pseudo t, ²J_{CH} = 3.9 Hz, RuCCH₂Ru); 170.64 (pseudo q, ²J_{CH} = 6.8 Hz, MeC=O); 185.39, 186.36, 190.37, 191.79, 194.58, 195.31, 196.14 (br), 196.30 (8 s, Ru₃(C \equiv O)₉); 210.53 (pseudo t, AcOCH₂CRu). MS (DCI/NH₃): m/z 721 ([MNH₄]⁺); 644 ([MH⁺ - AcOH]⁺). IR (THF): $\nu_{\text{C}\equiv\text{O}}$ 2102 (w), 2077 (s), 2047 (vs), 2009 (s), 1998 (s), 1971 (sh, m), 1747 (br, m), 1589 (vw) cm⁻¹.

Alternative Route to 5b from [Ru₃(CO)₁₂], [PPN][Cl], and 1,4-Bis(tosyloxy)but-2-yne. 1,4-Bis(tosyloxy)but-2-yne (**1b**; 0.093 g, 0.236 mmol) was added to a solution of [PPN]-[Ru₃(μ -Cl)(CO)₁₀], prepared in situ from Ru₃(CO)₁₂ (0.300 g, 0.47 mmol) and [PPN][Cl] (0.270 g, 0.47 mmol) in THF (30 mL) (see above). After a few minutes, the solution turned brown, at which point the formation of the intermediate **15d** was checked by IR. After evaporation of the solvent, the crude product was analyzed by NMR in THF-*d*₆. IR (THF): $\nu_{\text{C}\equiv\text{O}}$ 2124 (vw), 2058 (m), 2027 (vs), 2008 (s), 1974 (m), 1908 (vw), 1829 (w), 1589 (vw) cm⁻¹. ¹H NMR (400 MHz, THF-*d*₆): δ 0.99 (²J_{CH} = 2.4 Hz; CH isomer 1); 1.01 (²J_{CH} = 2.4 Hz; CH isomer 2); 1.93 (²J_{CH} = 2.4 Hz; CH isomer 1); 1.94 (²J_{CH} = 2.4 Hz; CH isomer 2). ¹³C{¹H} NMR (100 MHz, THF-*d*₆): δ 43.74 (CH₂, isomer 1); 43.82 (CH₂, isomer 2); 128.83 (=C=, isomer 1); 131.17 (=C=, isomer 2); 193.34, 196.42, 197.15, 197.86, 198.46, 198.69, 200.93, 204.42, 216.43, 228.21 (9 s over a broad signal; RuCO). The above signal assignments were based on consistent cross-peaks in ¹H-¹³C HMBC and HMQC spectra (see main text). Signals of THF, PPN⁺, and grease impurities were omitted.

Alternatively, the THF solution was cooled to -78 °C, protonated with HBF₄ (0.032 mL, 0.235 mmol), and then evaporated to dryness at room temperature. The residue was dissolved in a few drops of dichloromethane and chromatographed over silica gel using pentane as eluent. The colored fraction contained a mixture of the allenyl complex **5b** and

$\text{Ru}_3(\text{CO})_{12}$. After evaporation of pentane, the residue was treated with acetone, from which $\text{Ru}_3(\text{CO})_{12}$ precipitated (0.028 g, 9%). Evaporation of the acetone filtrate afforded the allenyl complex **5b** (0.024 g, 8%).

Preparation of Complex 10d. $\text{Ru}_3(\text{CO})_{12}$ (0.600 g, 0.94 mmol) and $[\text{PPN}][\text{Cl}]$ (0.540 g, 0.94 mmol) were dissolved in THF (60 mL). The solution was stirred for 3 h at room temperature under CO bubbling via a needle in the solution, until the characteristic red color of the $[\text{PPN}][\text{Ru}_3(\mu\text{-Cl})(\text{CO})_{10}]$ salt was obtained. After addition of 1,4-dihydroxybut-2-yne (0.081 g, 0.94 mmol), the formation of $[\text{PPN}][\text{Ru}_3(\mu\text{-Cl})(\text{CO})_9(\mu\text{-HOCH}_2\text{CCCH}_2\text{OH})]$ was monitored by infrared spectroscopy. The solution was then cooled to -78°C , and 2 equiv. of $\text{HBF}_4\cdot\text{OEt}_2$ was syringed successively (2×0.128 mL, 2×0.94 mmol). The reaction medium was then concentrated to dryness at room temperature. Dichloromethane (30 mL) was added, and the resulting suspension was filtered. Complex **10d** was obtained as a pale yellow solid (0.369 g; 54%). IR (THF): $\nu_{\text{C}=\text{O}}$ 2140 (w), 2114 (w), 2070 (sh), 2059 (vs), 2003 (s, broad) cm^{-1} . FAB MS: m/z 644 (M^+); 616 ($[\text{M} - \text{CO}]^+$); 588 ($[\text{M} - 2\text{CO}]^+$); 560 ($[\text{M} - 3\text{CO}]^+$). ^1H NMR (200 MHz, CD_3CN ; $T = 293$ K): δ 4.48 and 5.06 (2 dd, 4H, $^2J_{\text{HH}} = 3.9$ Hz, $^5J_{\text{HH}} = 2.8$ Hz; diastereotopic $\text{H}_2\text{C}=\text{C}=\text{CH}_2$). ^1H NMR (300 MHz, CD_3CN ; $T = 238$ K): δ 4.49 and 5.06 (2 dd, 4H, $^2J_{\text{HH}} = 3.8$ Hz, $^5J_{\text{HH}} = 3.0$ Hz; ^{13}C satellites; $^1J_{\text{CH}} = 164$ Hz; diastereotopic $\text{H}_2\text{C}=\text{C}=\text{CH}_2$). $^{13}\text{C}\{^1\text{H}\}$ NMR (75 MHz, CD_3CN , $T = 238$ K): δ 43.00 (CH_2); 184.60 (medium; $(\text{Ru}(\text{CO})_2)$); 188.00 (medium; $(\text{Ru}(\text{CO})_2)$); 188.2 (intense; central $\text{Ru}(\text{CO})_3$); 191.60 (medium; $(\text{Ru}(\text{CO})_2)$). The equivalence of the central $\text{Ru}(\text{CO})_3$ carbonyl ligands is tentatively and preliminarily assigned from the relative intensities of the carbonyl ^{13}CO signals. The signal of the butatriene central carbon atoms was not detected. ^{19}F NMR (188 MHz, CD_3CN): δ -69.49, -70.30, -70.35 (BF_4^-). Two attempts to obtain elemental analysis gave erratic results: this is likely due to the poor stability of the complex, the purity of which is however supported by ^1H , $^{13}\text{C}\{^1\text{H}\}$ and J-mod- ^{13}C NMR spectra (Supporting Information).

Evaporation of the CH_2Cl_2 filtrate afforded a solid residue (0.728 g), containing $[\text{PPN}]^+$ cations, and a side product, the structure of which could not be determined. As complementary details, some of its spectroscopic data are given hereafter. IR (CH_2Cl_2): $\nu_{\text{C}=\text{O}}$ 2086 (m), 2080 (m), 2055 (s, sharp), 2017 (s) cm^{-1} . ^1H NMR (200 MHz, CDCl_3): δ 4.58 (dt, $J_{\text{HH}} = 13.8$ Hz, $J_{\text{HH}} = 2.0$ Hz, 1 H); 4.70 (d, $J_{\text{HH}} = 13.8$ Hz; 1 H); 4.77 (d, $J_{\text{HH}} = 2.0$ Hz, 2 H). ^{13}C NMR (62 MHz, CDCl_3): δ 68.55 (t, $^1J_{\text{CH}} = 150$ Hz); 81.00 (t, $^1J_{\text{CH}} = 153$ Hz); 117.5 (s).

Computational Methods

Full geometry optimization and vibrational analysis of the allenylm cobalt complex **2b** was performed at the B3PW91/6-31G* level using Gaussian98.⁴⁷ Single-point energy calculations were performed on the optimized structure **2b** at the B3PW91/6-31G*/DZVP(Co) level and on the X-ray crystal structure of **5b** at the B3PW91/6-31G*/DZVP(Ru) level using Gaussian98.⁴⁸ Visualization of frontier orbitals was performed using Molekel.⁴⁹

The frontier orbitals are involved in a quantity called the Fukui function $f(\mathbf{r})$, first introduced in the 1980s by Yang and

Parr^{21a} and defined as the partial derivative of the electronic density $\rho(\mathbf{r})$ with respect to the total number of electrons N at constant external potential $v(\mathbf{r})$. A Maxwell relation links the chemical potential μ and $f(\mathbf{r})$ as⁵⁰

$$f(\mathbf{r}) = (\partial\rho/\partial N)_v = (\partial\mu/\partial v(\mathbf{r}))_N$$

Reactivity indices to describe molecular reactivity have therefore been proposed to describe (i) the nucleophilic attack on the system

$$f^+(\mathbf{r}) = (\partial\rho/\partial N)^+_v$$

(ii) the electrophilic attack on the system

$$f^-(\mathbf{r}) = (\partial\rho/\partial N)^-_v$$

and (iii) the radical attack on the system

$$f^\theta(\mathbf{r}) = 1/2(f^+(\mathbf{r}) + f^-(\mathbf{r}))$$

Because the evaluation of these derivatives is quite complicated, a finite difference scheme has been proposed to evaluate $f(\mathbf{r})$

$$f^+(\mathbf{r}) = \rho_{N+1}(\mathbf{r}) - \rho_N(\mathbf{r})$$

$$f^-(\mathbf{r}) = \rho_N(\mathbf{r}) - \rho_{N-1}(\mathbf{r})$$

$$f^\theta(\mathbf{r}) = 1/2(\rho_{N+1}(\mathbf{r}) - \rho_{N-1}(\mathbf{r}))$$

involving the electronic density of the systems with $N+1$, N , and $N-1$ electrons, respectively.

A further approximation allows us to design the condensed Fukui functions $f(k)$, which are atomic reactivity indices in contrast to the previous local Fukui functions:

$$f^+(k) = -Q_{N+1}(k) + Q_N(k)$$

$$f^-(k) = -Q_N(k) + Q_{N-1}(k)$$

$$f^\theta(k) = 1/2(-Q_{N+1}(k) + Q_{N-1}(k))$$

The gross charge Q_k was calculated from a Mulliken population analysis.

The global hardness $\eta = 1/S$ (S = softness) has been evaluated using the finite-difference approximation (the $1/2$ factor is now omitted in recent publications):²²

$$\eta = 1/S = I - A$$

It has been calculated from energy differences involving the system under consideration (N electrons) and the corresponding reduced and oxidized species obtained by vertical ionization (i.e. with the same geometry):

$$\eta = 1/S = E_{N+1} + E_{N-1} - 2E_N$$

(48) Godbout, N.; Salahub, D. R.; Andzelm, J.; Wimmer, E. *Can. J. Chem.* **1992**, *70*, 560. Basis sets were obtained from the Extensible Computational Chemistry Environment Basis Set Database, as developed and distributed by the Molecular Science Computing Facility, Environmental and Molecular Sciences Laboratory, which is part of the Pacific Northwest Laboratory, P.O. Box 999, Richland, WA 99352, and funded by the U.S. Department of Energy. The Pacific Northwest Laboratory is a multi-program laboratory operated by Battelle Memorial Institute for the U.S. Department of Energy under Contract DE-AC06-76RLO 1830. Contact David Feller or Karen Schuchardt for further information.

(49) Flükiger, P. F.; Portman, S. Molekel 3.04; University of Geneva and CSCS/SCSC-ETHZ, Switzerland, 1999.

(50) Parr, R. G.; Yang, W. *Density-Functional Theory of Atoms and Molecules*; Oxford University Press: New York, 1989.

(47) Frisch, M. J.; Trucks, G. W.; Schlegel, H. B.; Scuseria, G. E.; Robb, M. A.; Cheeseman, J. R.; Zakrzewski, V. G.; Montgomery, J. A., Jr.; Stratmann, R. E.; Burant, J. C.; Dapprich, S.; Millam, J. M.; Daniels, A. D.; Kudin, K. N.; Strain, M. C.; Farkas, O.; Tomasi, J.; Barone, V.; Cossi, M.; Cammi, R.; Mennucci, B.; Pomelli, C.; Adamo, C.; Clifford, S.; Ochterski, J.; Petersson, G. A.; Ayala, P. Y.; Cui, Q.; Morokuma, K.; Malick, D. K.; Rabuck, A. D.; Raghavachari, K.; Foresman, J. B.; Cioslowski, J.; Ortiz, J. V.; Stefanov, B. B.; Liu, G.; Liashenko, A.; Piskorz, P.; Komaromi, I.; Gomperts, R.; Martin, R. L.; Fox, D. J.; Keith, T.; Al-Laham, M. A.; Peng, C. Y.; Nanayakkara, A.; Gonzalez, C.; Challacombe, M.; Gill, P. M. W.; Johnson, B. G.; Chen, W.; Wong, M. W.; Andres, J. L.; Head-Gordon, M.; Replogle, E. S.; Pople, J. A. *Gaussian 98*, revision A.7; Gaussian, Inc.: Pittsburgh, PA, 1998.

Acknowledgment. We are indebted to Prof. Michael McGlinchey for stimulating discussions and useful suggestions, to Cécile Destombes, Antonetta Mohanu, and Tal Perry for experimental assistance, to Dr. Yannick Coppel for recording 2D-NMR spectra, and to Philippe Arnaud for computational assistance. We also wish to thank the Ministère de l'Education Nationale de la Recherche et de la Technologie for financial

support, and CALMIP (CALcul intensif en MIdi-Pyrénées, Toulouse, France) for computational facilities.

Supporting Information Available: Crystallographic data for compounds **3**, **5b**, and **8a**, including tables of crystal data, atomic coordinates, bond lengths and angles, and anisotropic thermal parameters and figures giving ^1H and $^{13}\text{C}\{^1\text{H}\}$ NMR spectra of complex **9a**, the ^1H NMR spectrum of complex **10b** and ^1H , $^{13}\text{C}\{^1\text{H}\}$, and J-Mod- ^{13}C NMR spectra of complex **10d**. This material is available free of charge via the Internet at <http://pubs.acs.org>.

OM010568W

(51) Maurette, L.; Godard, C.; Frau, S.; Lepetit, C.; Soleilhavoup, M.; Chauvin, R. *Chem. Eur. J.* **2001**, *7*, 1165.